Preprint

Enhancer RNAs are necessary and sufficient for activity-dependent neuronal gene transcription

Nancy V.N. Carullo[1], Rhiana C. Simon[1], Aaron J. Salisbury[1], Jasmin S. Revanna[1], Kendra D. Bunner[1], Katherine E. Savell[1], Faraz A. Sultan[1], Charles A. Gersbach[2], & Jeremy J. Day[1]*

Enhancer elements in DNA regulate gene expression programs important for neuronal fate and function, and are increasingly implicated in brain disease states. Enhancers undergo bidirectional transcription to generate non-coding enhancer RNAs (eRNAs), but the function of eRNAs in neuronal systems remains controversial. Here, we performed genome-wide characterization of transcribed enhancers from rat cortical neurons, revealing elevated sequence conservation, enriched localization near genes involved in neuronal or synaptic function, and correlated activity-dependent regulation of putative eRNA-mRNA pairs. Functional validation using a CRISPR-dCas9 fusion system to drive eRNA synthesis from enhancers produced corresponding increases in mRNA at linked genes. Focusing on eRNAs arising from enhancers at the *Fos* gene locus, we report that eRNA and mRNA correlate on a single-cell level, that CRISPR-targeted eRNA delivery to an enhancer is sufficient for mRNA induction, and that eRNA knockdown decreases mRNA and alters neuronal physiology. These results suggest that eRNAs regulate gene expression and neuronal function.

Correspondence to Jeremy Day (jjday@uab.edu | day-lab.org | @DayLabUAB)

TO ORCHESTRATE the precise gene expression patterns that give rise to the phenotypic and functional diversity of complex biological systems, mammalian genomes utilize millions of regulatory elements known as enhancers. These enhancers, often located many kilobases from genes that they regulate, direct transcriptional dynamics at linked genes by activation of proximal gene promoters (Heinz et al., 2015; Li et al., 2016; Wang et al., 2011). Enhancer-promoter interactions help to ensure the exquisite specificity of cell- and tissue-specific gene expression profiles in the brain, defining which genes can be turned on during neuronal specification and which genes remain accessible in adult neurons (Gray et al., 2015; Nord et al., 2013). In addition to regulating neuronal development, enhancer regions direct activity- and experience-dependent gene expression programs required for neuronal plasticity, memory formation, and behavioral adaptation to environmental stimuli (Joo et al., 2016; Kim et al., 2010; Malik et al., 2014; Schaukowitch et al., 2014; Telese et al., 2015). Moreover, the vast majority of DNA sequence variants that possess a causal relationship to neuropsychiatric disease and intellectual disability fall in non-coding regions of DNA (Davidson et al., 2011; Eckart et al., 2016; Edwards et al., 2012; Gordon and Lyonnet, 2014; Inoue and Inoue, 2016; Network and Pathway Analysis Subgroup of Psychiatric Genomics, 2015; Roussos et al., 2014; Schizophrenia Working Group of the Psychiatric Genomics, 2014; Vermunt et al., 2014; Voisin et al., 2015; Yao et al., 2015), and these variants are increasingly becoming linked to altered enhancer function. Thus, understanding how genomic enhancers regulate individual genes in neuronal systems is critical for unraveling transcriptional contributions to brain health and disease.

Recent advances in DNA sequencing have revealed that the transcriptional landscape of all mammalian organisms is far more complex than previously appreciated. In contrast to earlier predictions, a significant fraction of mammalian genomes is transcribed into non-coding RNAs, which include long non-coding RNAs (lncRNAs; generally defined as non-coding RNAs longer than 200 nucleotides) (Djebali et al., 2012; Hangauer et al., 2013; Quinn and Chang, 2016). Much of this lncRNA landscape is dedicated to enhancer regions which undergo bidirectional, RNA polymerase II (RNAP2)-dependent transcription to yield enhancer RNAs (eRNAs) that are generally not spliced or polyadenylated (Arner et al., 2015; Gray et al., 2015; Kim et al., 2015; Kim et al., 2010; Kim and Shiekhattar, 2015). Critically, RNA synthesis from enhancers that regulate cellular differentiation and responses to cellular activation occurs *prior* to mRNA synthesis from linked genes (Arner et al., 2015), and also *prior* to important chromatin remodeling events that are generally used to identify enhancers (Kaikkonen et al., 2013). In addition, eRNA transcription from enhancers is highly correlated with overall enhancer activity and the presence of enhancer-promoter loops (Li et al., 2016; Sanyal et al., 2012). In neuronal systems, eRNAs arising from activity-dependent enhancers are pervasively transcribed in response to neuronal activation, plasticity-inducing stimulation, and behavioral experience (Joo et al., 2016; Kim et al., 2010; Malik et al., 2014; Schaukowitch et al., 2014; Telese et al., 2015), providing a key link between enhancers and the downstream gene expression programs that regulate brain function.

Although recent reports suggest a functional role for eRNAs in regulation of enhancer states, the specific nature of this role is controversial. Here, we investigate eRNA transcription from neurons genome-wide as well as eRNA synthesis, localization, and function from well-characterized enhancers near the *Fos* gene. This immediate-early gene

[1]*Department of Neurobiology & Evelyn F. McKnight Brain Institute, University of Alabama at Birmingham, Birmingham, AL 35294, USA*
[2]*Department of Biomedical Engineering, Duke University, Durham, NC 27708, USA.*
**Corresponding author*

is broadly responsive to neuronal activity in the brain, and enhancers at this gene contribute to distinct activity-dependent induction dynamics of *Fos* mRNA (Fleischmann et al., 2003; Joo et al., 2016; Kim et al., 2010; Malik et al., 2014; Savell et al., 2016; Zovkic et al., 2014). We provide four lines of novel converging evidence supporting a critical functional role of eRNAs in neuronal systems. We show that activity-induced expression of eRNAs from enhancers is significantly correlated with expression from nearby activity-responsive genes across the genome, that *Fos* eRNAs are localized to distinct loci within the nucleus, and that eRNAs from a distal *Fos* enhancer are both necessary and sufficient for activity-regulated induction of *Fos* mRNA. Finally, we confirm the relevance of eRNAs in neuronal function by demonstrating that altered levels of a single eRNA can lead to decreased neuronal firing.

RESULTS

Neuronal stimulation reveals activity-dependent enhancer RNAs

To map neuronal eRNAs across the rat genome, we took advantage of the fact that eRNAs are predominantly non-polyadenylated transcripts. Using a recently published non-PolyA RNA-seq dataset from rat cortical neuron cultures (Savell et al., 2016), we quantified 12,924 regions of contiguous non-PolyA transcription that fell >1kb outside of annotated gene boundaries, consistent with common cutoffs used to dissociate enhancers from more proximal promoters (**Fig. 1A**). To ensure that these transcribed regions were in fact enhancers, we utilized publicly available ENCODE datasets from adult mouse cortex for the major histone modifications associated with enhancer loci (H3K4me1, H3K4me3, and H4K27ac). Of 12,924 transcribed intergenic regions (TIRs), 3,107 regions overlapped H3K4me1 peaks (a mark of active enhancers (Li et al., 2016)) or overlapped both H3K4me3 and H4K27ac peaks (marks often used to denote poised enhancers (Li et al., 2016)). These transcribed regions, which we designated as transcriptionally active enhancers (TAEs; **Fig. 1A-B**), exhibited increased levels of non-polyA RNA expression as compared to non-enhancer TIRs (data not shown), and were also enriched for RNA Polymerase II (RNAP2) and the enhancer-linked chromatin looping factor CTCF (CCCTC-binding factor) (**Fig. 1B**). DNA sequences at these locations exhibited elevated sequence conservation and overlap with CpG islands, regions which generally lack DNA methylation (another cardinal feature of enhancers). Gene-ontology analysis revealed an enrichment in terms associated with neurodevelopment, synapse dynamics, and overall neuronal function for genes adjacent to TAEs (**Fig. 1C**).

To determine whether eRNAs are correlated with activity-dependent alterations in protein-coding genes, we examined non-PolyA RNA transcription from TAEs following neuronal depolarization with 25mM potassium chloride (KCl). Previous studies have shown differential, stimulus-dependent induction of eRNAs. While in this study different enhancers displayed different expression patterns dependent on specific activation stimuli, all enhancers tested showed robust eRNA induction in response to KCl-mediated depolarization (Joo et al., 2016). This allowed us to investigate both eRNA and mRNA expression changes (from distinct PolyA+ RNA datasets) in response to neuronal depolarization. We identified over 230 genes (termed immediate early genes, or IEGs; **Supplementary Data Table 1**) and 89 TAEs (termed activity-regulated TAEs, or arTAEs) that were significantly altered by KCl treatment. To examine correlations in depolarization-induced changes at individual eRNA-mRNA pairs, we annotated the nearest IEG (within 1Mbp) to each of the 89 arTAE loci (**Fig. 1D**; **Supplementary Data Table 2**). 42% of arTAEs met this criterion, and at these loci, activity-induced expression of eRNAs and mRNAs were significantly correlated. **Figure 1E-G** shows non-PolyA RNA-seq results from three representative IEGs (*Arc*, *Nr4a1*, and *Fos*) that are significantly induced by KCl depolarization. Each of these genes displayed distal arTAEs, including at least 3 distinct enhancers near the *Fos* gene. The locations of these enhancers are consistent with locations of enhancer elements in other species relative to the *Fos* gene (Joo et al., 2016; Kim et al., 2010), and map to DNA sequences that are enriched for RNAP2 and histone modifications associated with active enhancers (H3K4me1 and H3K27ac). Further, each of these elements undergoes bidirectional transcription to yield strand-specific eRNAs.

Validation of enhancer function using CRISPRa

To determine whether transcriptional activation at selected candidate enhancers was sufficient to induce mRNA at linked genes, we employed a CRISPR-dCas9 activation (CRISPRa) system in which dCas9 is fused to a strong transcriptional activator (such as VPR or VP64), allowing selective activation of targeted genomic sites (**Fig. 2A**). We designed CRISPR guide RNAs (gRNAs) to target our CRISPRa system to enhancer sites surrounding the *Fos*, *Fosb*, and *Nr4a1* genes, as well as gRNAs targeting the respective promoters to drive mRNA expression directly (**Fig. 2**, **Fig. S2**). In addition, we constructed a guide RNA for *LacZ*, a bacterial gene that is not present in eukaryotes, as a non-targeting control.

On DIV4-5, cortical cultured neurons were transduced with separate lentiviruses containing dCas9-VPR and guide RNA constructs. On DIV11, we confirmed transgene expression (indicated by mCherry reporter for gRNA constructs and FLAG immunocytochemistry for the VPR construct; **Fig. 2B**) and extracted RNA for RT-qPCR. At all four candidate eRNA-mRNA pairs, CRISPR-VPR mediated transcriptional activation of enhancers not only increased eRNA expression, but also significantly induced corresponding mRNA levels. In contrast, dCas9-VPR targeting of gene promoters specifically increased target mRNA at all candidate genes, but did not alter eRNA levels at three out of four candidate pairs (**Fig. 2C-E**). For example, activation of distinct enhancers either upstream (enhancer-1) or downstream (enhancer-3) at the *Fos* gene, produced local eRNA (eRNA-1 and eRNA-3) induction, but also significantly increased *Fos* mRNA expression. Notably, transcriptional activation of the upstream enhancer did not activate the downstream enhancer, and vice versa (**Fig. 2C**). This strongly indicates that enhancers and eRNAs can be induced by transcriptional activators, that this activation can drive mRNA expression, and that there is little crosstalk between enhancers. Interestingly, dual activation of the two enhancers with multiplexed sgRNAs targeting *Fos* enhancer-1 and enhancer-3 had additive effects and stronger mRNA induction compared to individual enhancer activation (**Fig. S1**). Given that enhancers can interact with promoters in enhancer enhancer-promoter loops, it is possible that transcriptional activators are close enough to act simultaneously on enhancers and promoters. However, we observed little or no effect on eRNA expression when we targeted gene promoters to drive mRNA expression (**Fig.**

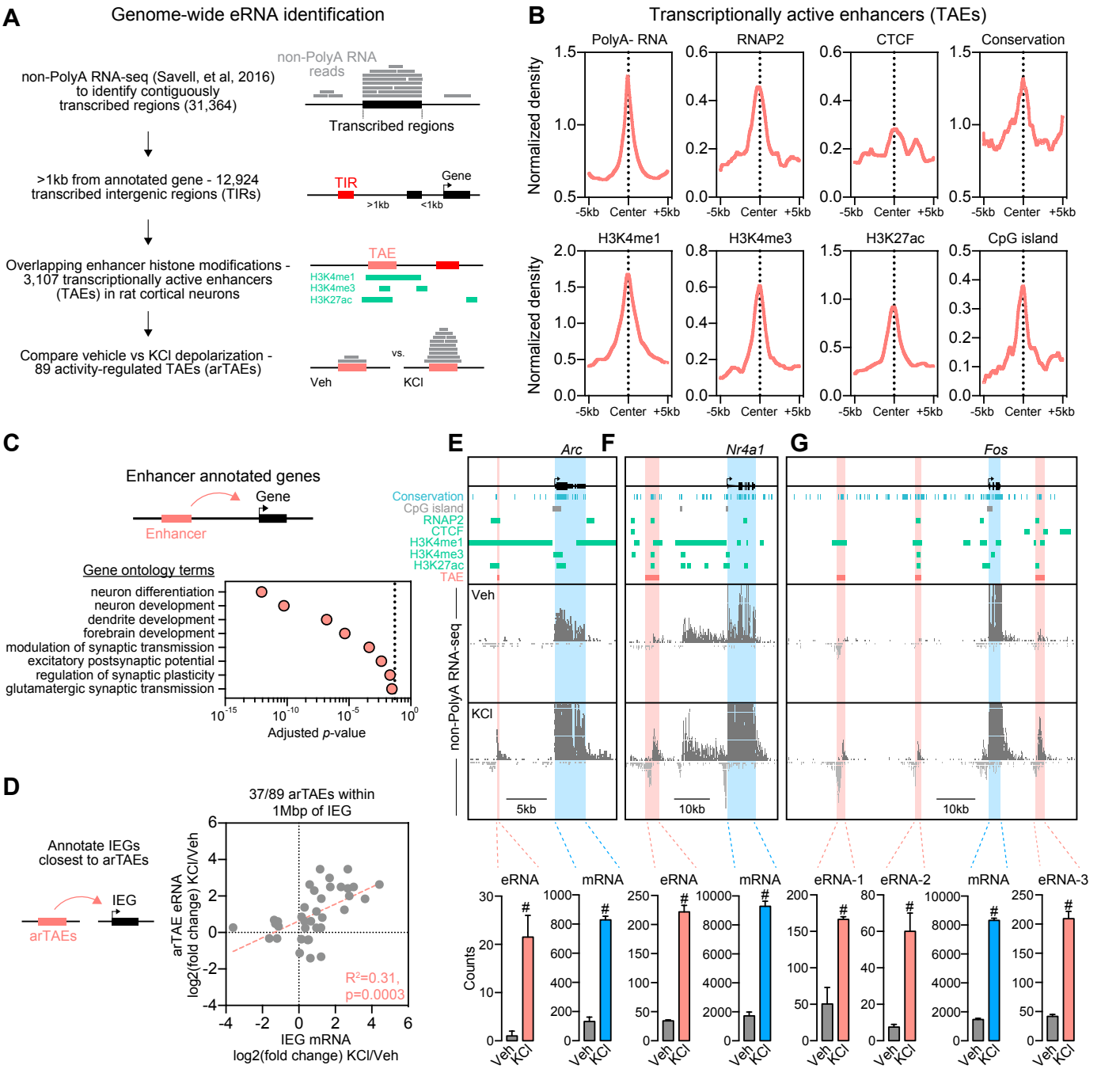

Figure 1. Genome-wide characterization of eRNAs. **A**, Analysis pipeline for localization and quantification of transcriptionally active enhancers (TAEs), and genome-wide comparisons of eRNA expression following neuronal depolarization. Non-PolyA RNA-seq datasets from previous publication using cultured rat cortical neurons (Savell, et al., 2016) were used to identify contiguously transcribed regions, which were filtered to remove transcribed regions overlapping annotated genes. Of 12,924 transcribed intergenic regions (TIRs), 24% (3,107 loci) overlapped histone modifications consistent with active or poised enhancers, and were designated TAEs. Of these, 89 met genome-wide criteria for differential expression following 1hr neuronal depolarization with 25 mM potassium chloride (KCl), and were designated activity-regulated TAEs (arTAEs). **B**, Transcriptionally active enhancers exhibit elevated RNAP2 occupancy, CTCF binding, sequence conservation (phastCons13way score), histone modifications (H3K4me1, H3K4me3, H3K27ac), and CpG island density as compared to surrounding regions. Chromatin immunoprecipitation datasets were obtained from the adult mouse cortex (ENCODE project) and lifted over to the rat Rn5 genome assembly. **C**, Gene ontology for 1,362 unique genes closest to TAEs. TAEs are enriched near genes that regulate neuronal function and synaptic transmission. **D**, eRNA-mRNA pairs were determined by annotation of closest immediate early genes (IEGs) induced by neuronal depolarization with 25 mM KCl, with a 1Mbp distance cutoff. Correlation between differential expression of IEG mRNAs following KCl depolarization and differential expression of eRNA from closest arTAEs following depolarization. Values are expressed as log2(fold change) of eRNA or mRNA counts used for comparison in DESeq2. Correlation determined with linear regression. **E-G**, Top, Genome browser tracks showing Non-PolyA RNA expression at three KCl-regulated IEGs (*Arc*, *Nr4a1*, and *Fos*), relative to tracks marking conserved DNA elements, CpG islands, RNAP2 and CTCF binding, and enhancer-linked histone modifications. Our pipeline identified one or more TAEs near each IEG. Bottom, RNA-seq count quantification of transcripts from TAEs (eRNAs in pink, from non-PolyA libraries), and mRNAs (in blue, from separate PolyA+ libraries). #FDR < 0.05 for DeSeq2 comparison of differential expression between vehicle and KCl groups.

2C-F), suggesting that eRNA regulation of linked mRNA is typically a unidirectional phenomenon. Moreover, we did not observe any effects of enhancer activation on non-targeted eRNAs or mRNAs, supporting the site-specificity of the observed CRISPRa effects (**Fig. 2F**).

To determine whether these results translate to non-neuronal cell types, we repeated selected experiments in C6 cells, a rat glioma dividing cell line (**Fig. S2**). As in neurons, we found that recruitment of transcriptional activators (VPR or VP64) to selected *Fos* enhancers not only induced transcription at enhancers but also upregulated *Fos* mRNA. In contrast, *Fos* promoter targeting with dCas9-

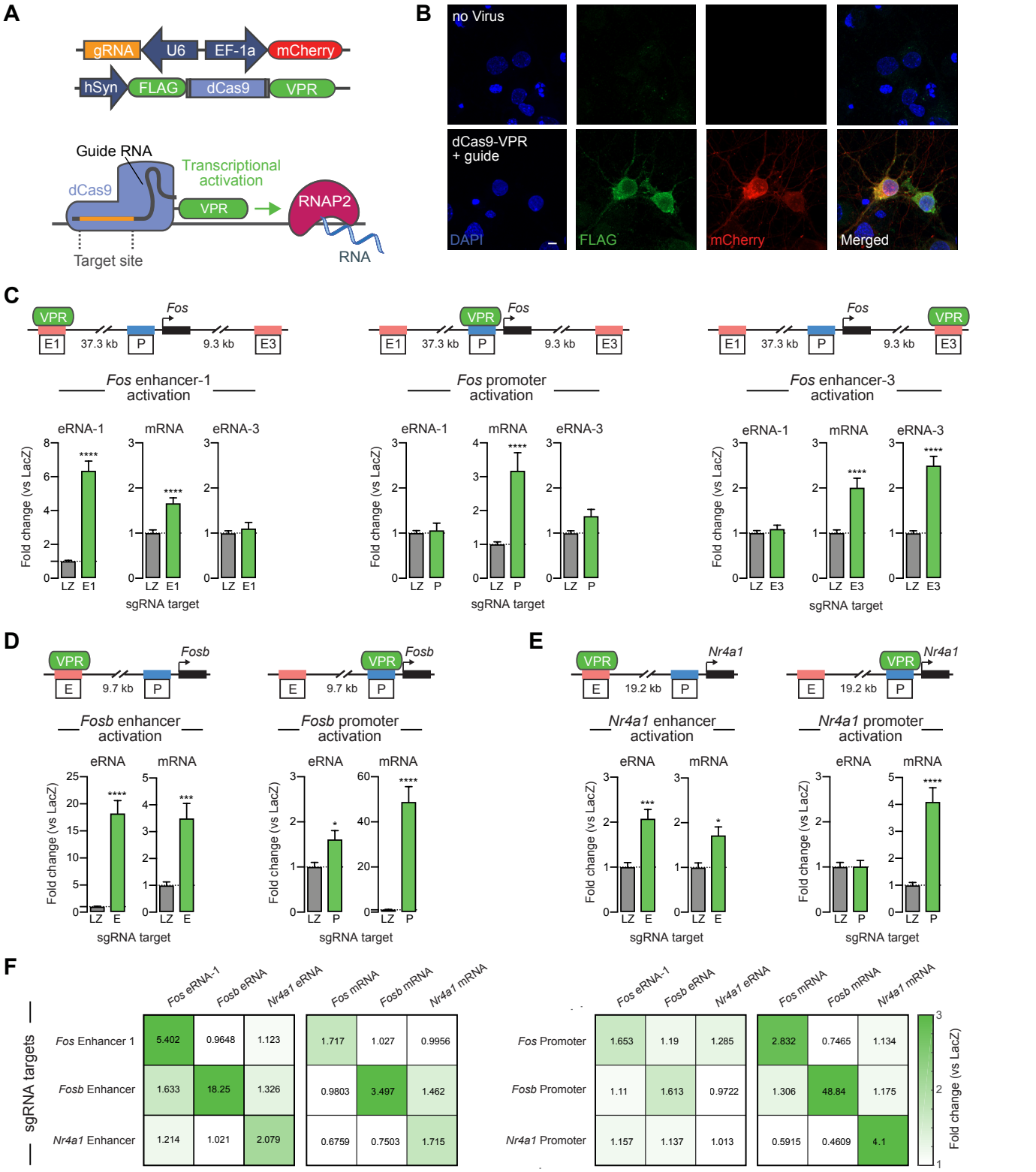

Figure 2. Transcriptional activation at enhancers is sufficient to induce linked genes. **A**, Illustration of CRISPR activation (CRISPRa) strategy for site-specific targeting of the transcriptional activator VPR. **B**, Immunocytochemistry on DIV11 neurons. Top, no virus control. Bottom, neurons co-transduced with lentiviruses expressing dCas9-VPR (marked by FLAG) and a custom sgRNA (mCherry reporter). Scale bar = 5 μm. **C**, CRISPRa targeting at a distal upstream enhancer (left panel), the proximal promoter (middle panel), or a downstream enhancer (right panel) at the *Fos* gene locus. VPR targeting to enhancers induced robust eRNA transcription and also increased mRNA levels, whereas *Fos* promoter targeting elevated mRNA but did not induce eRNA transcribed from either enhancer. Gene expression differences were measured with RT-qPCR (n=9-18 per group; two-tailed Mann-Whitney test for all comparisons), and all manipulations are compared to a non-targeting sgRNA control (LacZ, a bacterial gene not found in the mammalian genome). **D-E**, VPR mediated induction of *Fosb* and *Nr4a1* enhancers increased eRNA and mRNA expression while promoter activation resulted in mRNA induction, compared to the non-targeting LacZ (LZ) control (n=9 per group; two-tailed Mann-Whitney test for all comparisons). **F**, RT-qPCR data heatmap of CRISPRa experiments demonstrating specificity of enhancer (left) and promoter (right) activation. Enhancer activation induced eRNAs and mRNAs at the target genes with little effect on other tested eRNA or mRNAs. Promoter activation produced increases in mRNA with little effect on eRNA levels. Data expressed as mean ± s.e.m. Multiple comparisons, *p<0.05, **p<0.01, ***p<0.001, ****p<0.0001.

VPR or dCas9-VP64 elevated mRNA levels without altering eRNA levels. Finally, to determine whether establishment of key enhancer-linked histone modifications is sufficient to induce eRNA transcription and upregulate linked genes, we targeted dCas9 fused to p300 (a histone acetyltransferase and transcriptional co-activator) to *Fos* enhancer-1. As with VPR and VP64 targeting, p300 induced *Fos* eRNA-1 transcription and also elevated *Fos* mRNA (**Fig. S3**). Together, these findings imply that enhancers can be activated in a site-specific manner and that observed increases in mRNA are in fact the result of enhancer activation and potentially increased eRNA levels.

Fos enhancer RNAs are induced by diverse stimuli and require RNA Polymerase II

To determine whether *Fos* eRNAs are sensitive to other forms of neuronal and synaptic sensitive to other forms of neuronal and synaptic activation or inactivation, DIV 11 cortical neurons were stimulated with specific glutamate receptor agonists (AMPA and NMDA), the adenylyl cyclase activator Forskolin, or inactivated with the sodium channel blocker tetrodotoxin (TTX) (**Fig. 3A**). Here, we focused on enhancer RNA transcribed from the most distal and most conserved *Fos* enhancer and found increased transcription of eRNA-1 in response to KCl, AMPA, NMDA, and Forskolin in a dose-dependent fashion. Likewise, *Fos* eRNA-1 levels were reduced by TTX, suggesting that eRNA levels at this gene are bidirectionally modulated by neuronal activity states. To further explore this relationship, we performed a KCl stimulation time-course experiment in which cultured neurons were depolarized with KCl and RNA was isolated from neurons at multiple time points (15, 30, 45, and 60 min) after treatment. These results revealed that *Fos* eRNA-1 is upregulated as soon as 15 min following KCl depolarization, whereas *Fos* mRNA is not significantly upregulated until 30 min after stimulation (**Fig. 3B**). Moreover, *Fos* eRNA expression plateaus at 45 min after neuronal depolarization, whereas *Fos* mRNA levels continue to rise. These results indicate *Fos* eRNA is induced prior to *Fos* mRNA following neuronal activation and confirm previously described dynamics of eRNA transcription (Schaukowitch et al., 2014; Arner et al., 2015).

To examine the mechanisms responsible for synthesis of *Fos* eRNA-1, we next performed chromatin immunoprecipitation (ChIP) for RNAP2 following KCl depolarization. KCl- induced *Fos* eRNA-1 transcription was associated with significant recruitment (roughly 2-fold increase) of RNAP2 at the *Fos* enhancer-1 locus, as well as an expected increase at the *Fos* gene promoter (**Fig. 3C**). Moreover, pre-treatment with 5,6-dichloro-1-β-D-ribofuranosylbenzimidazole (DRB; a potent inhibitor of RNAP2-dependent transcription) prior to incubation with KCl resulted in significant blockade of KCl-induced expression of both *Fos* eRNA-1 and *Fos* mRNA (**Fig. 3D**). These results confirm that activity-dependent expression of *Fos* eRNA-1 is associated with RNAP2 recruitment and is dependent on RNAP2 activity for synthesis.

smFISH reveals correlation between Fos eRNA-1 and mRNA on a single cell level

To gain insight into the spatial distribution of eRNAs and their response to stimulation, we performed single molecule fluorescent in situ hybridization (smFISH), a technique that allows visualization of individual eRNA and mRNA transcripts on a single cell level. Using this tool, we investigated whether the number or localization of our RNA transcripts of interest changed in response to neuronal activation. Additionally, we investigated whether eRNA and mRNA expression are correlated across individual neurons. Cortical neurons were KCl-treated for 1 hr prior to fixation, permeabilization, and hybridization with fluorescently labeled smFISH probes. We designed custom probe sets to selectively target and mark individual *Gapdh* and *Fos* mRNA transcripts, as well as *Fos* eRNA transcripts arising from two enhancers (enhancer-1 and -3) upstream and downstream of the *Fos* gene (**Fig. 4A**). As shown in **Figure 4C-D**, the number of *Gapdh* transcripts was unaffected by neuronal depolarization while, as expected, the level of *Fos* mRNA signal increased in KCl-treated neurons. It is possible that this effect is stronger than represented in our analysis due to overlapping signal in neurons with high transcript abundance (which would potentially cause overlapping or nearby spots to be counted together). Interestingly, we detected only a few, but very discrete puncta per cell with both eRNA probe sets (*Fos* eRNA-1 and -3). Larger high-intensity foci are typically associated with active transcription sites as they indicate an accumulation of transcripts. We

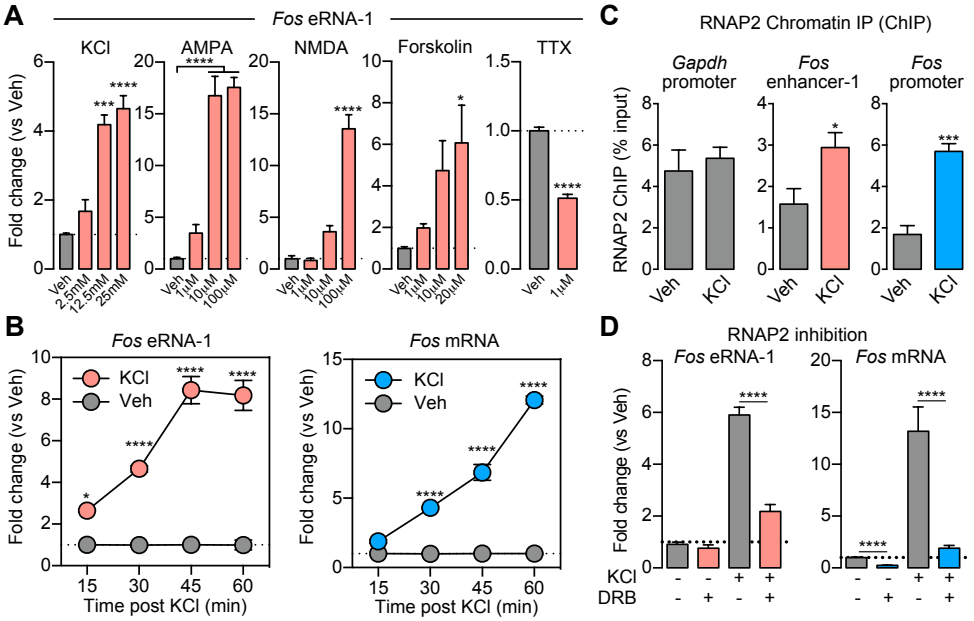

Figure 3. Activity-dependence and synthesis of *Fos* eRNAs. **A**, RT-qPCR analysis of eRNA-1 expression in response to 1h treatment with KCl, AMPA, NMDA, and Forskolin reveals activity dependent induction of *Fos* eRNA-1, while TTX treatment resulted in decreased *Fos* eRNA-1 expression (one-way ANOVA for KCl F(3,8)=39.05, p<0.0001, AMPA F(3,8)=59.04, p<0.0001, NMDA F(3,8)=61.87, p<0.0001, FSK F(3,8)=4.132, p<0.05, with Dunnette's post hoc test for multiple comparisons, and unpaired t-test for TTX t(10)=12.83, p<0.0001). **B**, *Fos* eRNA-1 is upregulated at 15 min and peaks after 45 min of KCl treatment (two-way ANOVA with main effect of KCl, F(3,15)=35.4, p<0.0001, Sidak's post hoc test for multiple comparison). In contrast, *Fos* mRNA is induced within 30 min and does not plateau within the 60 min time course (two-way ANOVA, F(3,16)=169.2, p<0.0001, Sidak's post hoc test for multiple comparison). **C**, RNAP2 CHIP reveals increased recruitment of RNAP2 to the *Fos* enhancer-1 and *Fos* promoter after KCl-mediated depolarization (unpaired t-test, for enhancer-1 t(6)=2.651, p<0.05, and promoter t(6)=7.812, p<0.001). **D**, 2 hr pre-treatment with RNAP2 dependent transcription inhibitor DRB prior to 1 h KCl treatment blocked KCl mediated induction of *Fos* eRNA-1 and mRNA (two-way ANOVA, with main effect of DRB F(1,42)=34.15, p<0.0001, and F(1,41)=84.64, Tukey's post hoc test for multiple comparison). Data expressed as mean ± s.e.m. Multiple comparisons, *p<0.05, **p<0.01, ***p<0.001, ****p<0.0001.

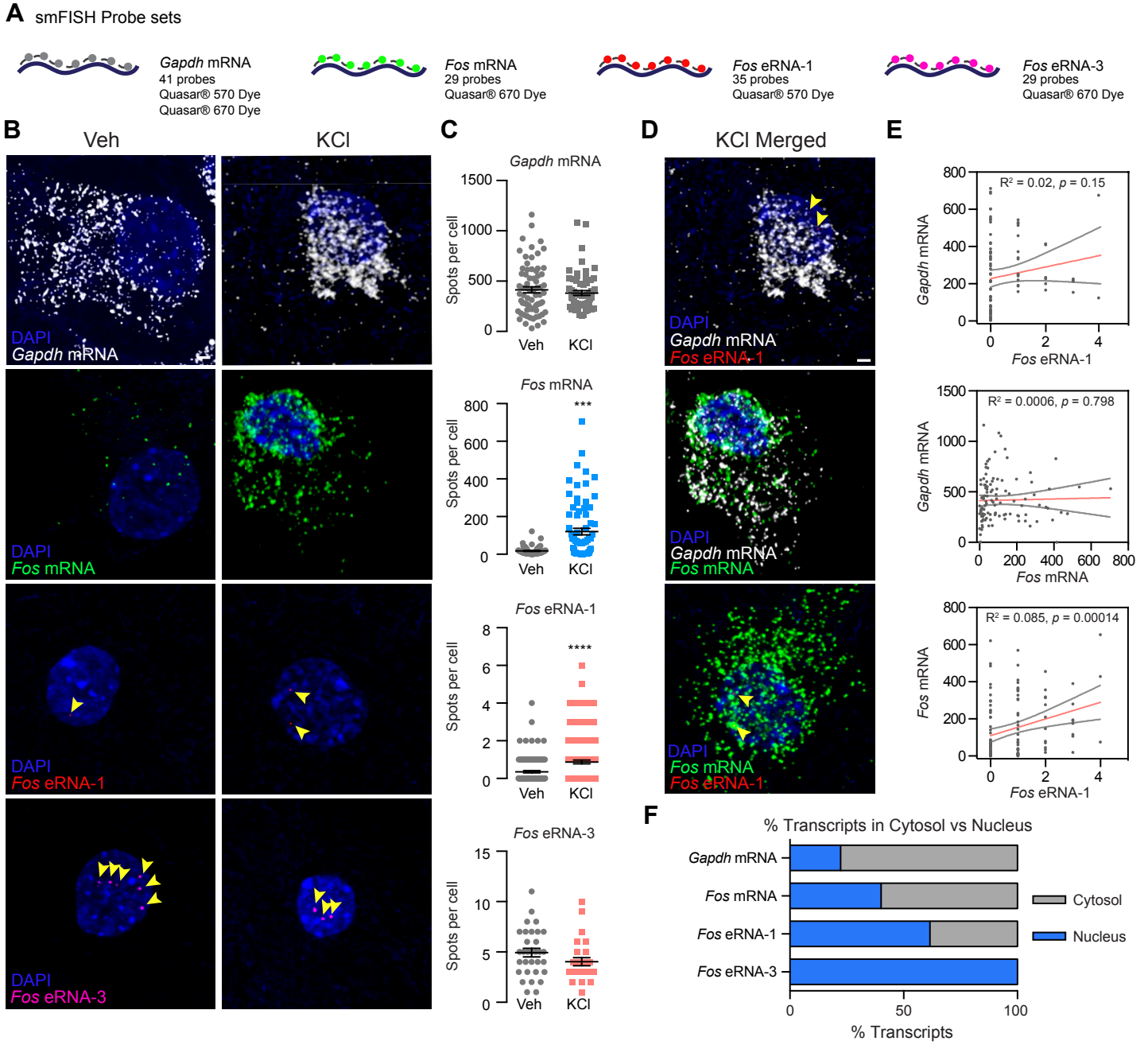

Figure 4. Cellular localization of *Fos* eRNA and mRNA. **A**, Illustration of smFISH probe sets indicating number of probes, dye, and LUT. **B,** smFISH for *Gapdh* mRNA (Quasar® 570), *Fos* mRNA (Quasar® 670), eRNA-1 (Quasar® 570) and eRNA-3 (Quasar® 670) transcripts at baseline and after KCl-mediated depolarization. Cell nuclei are stained with DAPI (blue), RNA transcripts are marked by smFISH probes (gray, green, red, and pink). Scale bar 2 μm. **C**, Quantification of spot detection using StarSearch. Number of detected spots for *Fos* mRNA and *Fos* eRNA-1 changes significantly after stimulation (Mann-Whitney test for Gapdh n(veh)=72, n(KCl)=63, U=2187, p>0.05; *Fos* mRNA n(veh)=77, n(KCl)=76, U=1929, p<0.001; eRNA-1 n(Veh)=124, n(KCl)=141, U=6540, p>0.0001; eRNA-3 n(veh)=32, n(KCl)=27, U=316.5, p>0.05). **D**, Merged KCl images of *Gapdh* mRNA, *Fos* mRNA and eRNA-1. **E**, Comparison and correlation of detected *Gapdh* mRNA, *Fos* mRNA and eRNA-1 spots per cell. There is a significant correlation between *Fos* mRNA (Quasar® 670) and *Fos* eRNA-1 (Quasar® 570) (Pearson r, R-square=0.08481, p=0.0014) but not between *Gapdh* mRNA (Quasar® 570) and *Fos* mRNA (Quasar® 670) or *Gapdh* mRNA (Quasar® 670) and eRNA-1 (Quasar® 570) (Pearson r for *Gapdh* mRNA and *Fos* mRNA R-square=0.000586, p=0.7982; *Gapdh* mRNA and eRNA-1 R-square=0.02344, p=0.1451). **F**, Quantification of smFISH for *Gapdh* mRNA, *Fos* mRNA, *Fos* eRNA-1 and *Fos* eRNA-3 transcripts in the cytosol vs nucleus. Data expressed as mean ± s.e.m. Multiple comparisons, *p<0.05, **p<0.01, ***p<0.001, ****p<0.0001.

observed this phenomenon frequently in the quantification of *Fos* mRNA signal, where active transcription is expected in response to depolarization. However, for eRNAs, we found such high-intensity puncta to occur much more frequently in both treatment groups, suggesting an accumulation of transcripts at these sites. If these bright punctae were true transcription sites, we would expect to detect up to two loci per nucleus. Surprisingly, both eRNAs intermittently displayed more than two transcript accumulation sites, indicating that eRNAs concentrate and potentially act at several specific loci within the nucleus or even at multiple different genes. In agreement with our RT-qPCR data (**Fig. 3A**), we detected significantly more *Fos* eRNA-1 puncta after KCl treatment compared to the vehicle group, which was close to the background signal (KCl: 0.8794 ± 0.1014 spots/cell, Veh: 0.3558 ± 0.06080 spots/cell, Quasar 570 channel background: 0.3761 ± 0.07906 spots/cell). Unexpectedly, we detected no change in *Fos* eRNA-3 punctae after KCl stimulation, despite the fact that non-Poly-A RNA seq (**Fig. 1**) revealed a KCl-induced increase in transcripts mapping to this enhancer. However, as suggested above, it is possible that eRNA-3 transcripts could accumulate at the overlapping

target locations, resulting in the same number of detected foci despite increased transcript abundance. Whether eRNA-1 and eRNA-3 are regulated differently and/or fulfill different functions remains to be elucidated. Our data, along with the literature, provide evidence for both sides. While general KCl-mediated depolarization activated all *Fos* enhancers and CRISPR-mediated targeted activation of individual *Fos* enhancers all resulted in increased mRNA expression (**Fig. 2**), it has been shown that the individual *Fos* enhancers can respond differently to various activation protocols (Joo et al., 2016). Likewise, eRNAs regulating other genes have been shown to have diverse binding partners and functions ((Bose et al., 2017; Hsieh et al., 2014; Lai et al., 2013; Li et al., 2013; Li et al., 2016; Schaukowitch et al., 2014; Sigova et al., 2015). However, it has not been tested whether enhancers from the same gene could have distinct functions. It is possible that different regulatory mechanisms determine eRNA induction to certain stimuli and signals to allow for a more fine-tuned response.

To determine whether eRNA and mRNA levels are correlated at the single-cell level, we multiplexed probe sets targeting *Gapdh* mRNA and *Fos* eRNA-1, *Gapdh* mRNA and *Fos* mRNA, or *Fos* eRNA-1 and *Fos* mRNA. There was no correlation between *Gapdh* mRNA punctae and either eRNA-1 or *Fos* mRNA counts, demonstrating that the number of *Fos* transcripts was not significantly related to other factors like cell size or health. Interestingly, these experiments also revealed a modest but significant correlation of *Fos* eRNA-1 and *Fos* mRNA transcript numbers on a single cell level (**Fig. 4D-E**). While punctae indicating eRNA transcripts were predominantly found in the nucleus, mRNA transcripts were detected in both the cytosol and nucleus (**Fig. 4F**). Taken together, these findings indicate that eRNAs contribute to transcriptional regulation of their target genes not only on a cell population level but also on a single cell level.

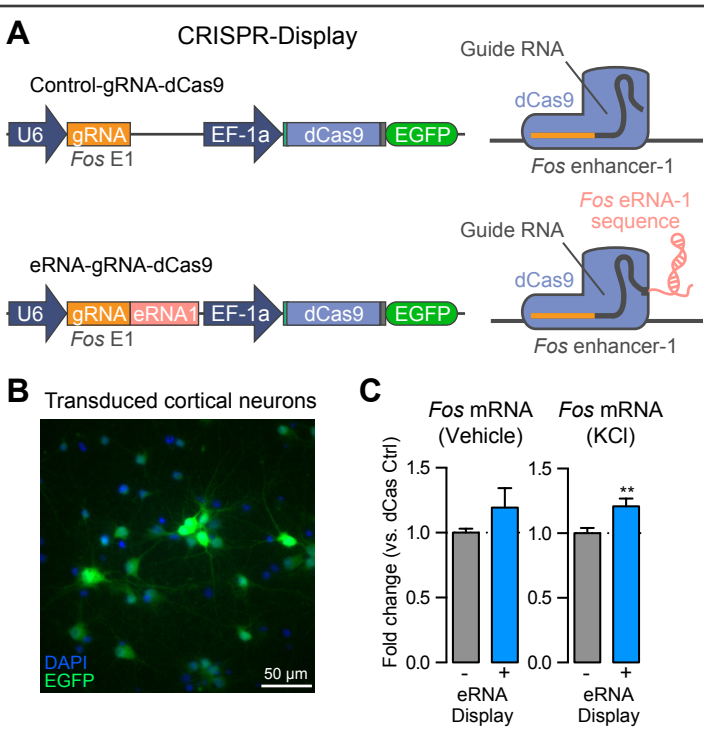

Figure 5. *Fos* eRNA-1 is sufficient for *Fos* mRNA expression in neurons. **A**, Illustration of CRISPR-Display strategy for *Fos* eRNA localization to *Fos* enhancer-1. *Fos* eRNA-1 sequence was expressed with specific guide RNAs to target selected enhancers. **B**, Cultured cortical neurons transduced with lentivirus containing *Fos* eRNA-1 CRISPR-Display construct. Neurons were transduced at 4DIV and IHC with anti-GFP antibodies was performed at 11DIV. **C**, RT-qPCR analysis reveals that targeting eRNA-1 to enhancer-1 results in stronger *Fos* mRNA induction upon activation, but not at baseline (n=9 per group, Mann-Whitney test Baseline U=28, p=0.29, and Activation U=11.50, p<0.01). Data expressed as mean ± s.e.m. Multiple comparisons, *p<0.05, **p<0.01, ***p<0.001, ****p<0.0001.

Enhancer RNAs are sufficient and necessary for induction of mRNA

Considering that the mechanisms by which eRNA can regulate proximal mRNA transcription is widely unknown, we explored the effect of localized eRNAs on the expression of linked genes. To do so, we employed CRISPR-Display (Shechner et al., 2015), a novel CRISPR approach that allowed us to tether a specific eRNA sequence to chosen target sites in the genome and investigate local effects, as compared to global over-expression approaches. Given that induction of eRNAs from *Fos* enhancer-1 showed high sequence conservation and robust effects on mRNA expression in neurons as well as in C6 cells, we selected a Display accessory-RNA sequence based on a conserved region within this particular enhancer element (**Fig. 5A**, **Fig. S4**). We packaged dCas9 along with either a gRNA-eRNA (eRNA-tethering Display construct) or gRNA-alone (control construct) cassette into a lentivirus. Both constructs contained the same gRNA targeting *Fos* enhancer-1. On DIV4, we transduced primary rat cortical neuronal cultures with either control virus or a virus expressing the eRNA-tethering Display construct (**Fig. 5B-C**). Following a 7-day incubation period to allow for sufficient viral expression, cells underwent a 1 hr vehicle or KCl treatment prior to RNA extraction and RT-qPCR on DIV 11. Anchoring of this eRNA-1 based sequence in close proximity to enhancer-1 resulted in stronger *Fos* mRNA induction in response to KCl-mediated neuronal depolarization (**Fig. 5C**). The same eRNA-tethering CRISPR-Display construct also achieved an increase in *Fos* mRNA expression at baseline in nucleofected C6 cells (**Fig. S4**). Taken together, these results support a model in which eRNAs act locally on a genomic region to facilitate transcriptional induction. More importantly, these experiments provide novel evidence that *Fos* eRNA-1 is sufficient to induce the *Fos* gene and enhance mRNA transcription in response to a stimulus.

To further interrogate the functional role of eRNAs in activity-dependent gene transcription in cortical neurons, we employed an anti-sense oligonucleotide (ASO) strategy to directly target eRNAs while leaving mRNA and other enhancer functions unperturbed. Rat primary cortical cultures were treated with sequence-specific eRNA-1 ASOs for 24 hrs prior to RNA harvesting followed by RT-qPCR (**Fig. 6A**). ASOs targeted to *Fos* eRNA-1 induced a robust decrease in eRNA-1 expression but did not alter expression of eRNAs from other *Fos* gene enhancers (again suggestive of functional independence of *Fos* eRNAs). Notably, *Fos* eRNA-1 ASOs also produced a significant decrease in *Fos* mRNA levels, both at baseline and following neuronal depolarization with KCl (**Fig. 6A-C**). These results suggest that *Fos* eRNA-1 is required for normal expression from the *Fos* gene, and that eRNA-1 is required for neuronal activation to induce expression of this immediate early gene. In contrast, we found that knockdown of *Fos* mRNA with a distinct targeted ASO had no effect on eRNA synthesis from any enhancer, further supporting a unidirectional model of eRNA function (**Fig. 6B**).

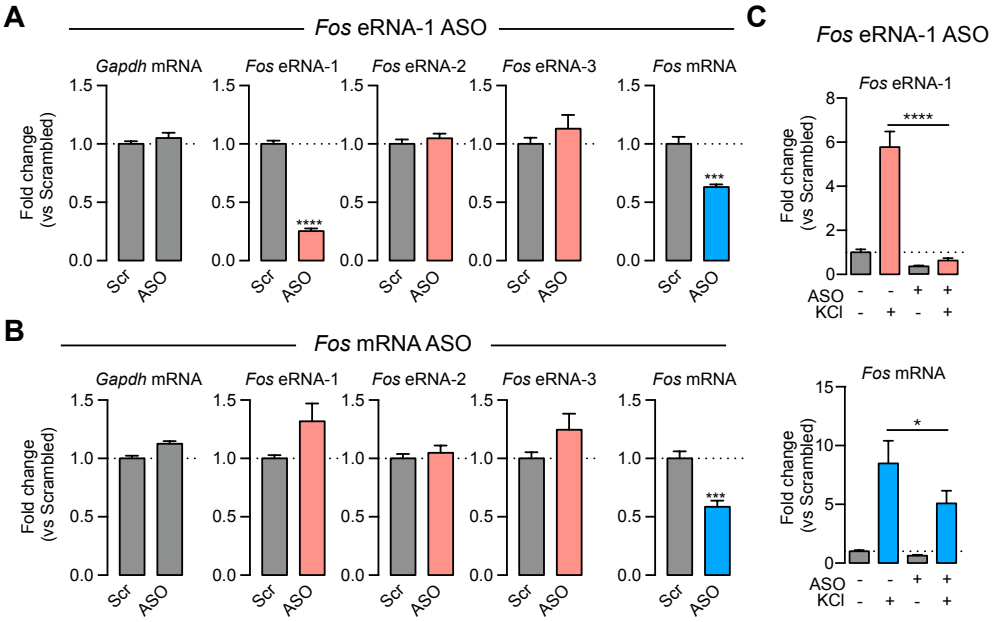

Figure 6. *Fos* eRNA-1 is necessary for *Fos* mRNA expression in neurons. **A**, Anti-sense oligonucleotide (ASO) targeting of *Fos* eRNA-1 for 24hrs decreased both eRNA-1 and *Fos* mRNA (unpaired t-test t(10)=20.69, p<0.0001 and t(10)=5.739, p<0.001), but did not alter eRNA levels from other *Fos* enhancers. **B**, *Fos* mRNA targeting ASOs decreased mRNA (t(10)=5.198, p<0.001) with no significant effect on eRNA levels. **C**, 24 hr *Fos* eRNA-1 ASO pretreatment prior to 1h KCl stimulation reduced induction of eRNA-1 (top) and mRNA (bottom) in response to depolarization when compared to a scrambled ASO control (unpaired t-tests, Veh eRNA-1: t(16)=4.332, p=0.0005; Veh mRNA: t(16)=2.454, p=0.0295; KCl eRNA-1: t(16)=17.12, p<0.0001; KCl mRNA: t(16)=3.772, p=0.0017). Data expressed as mean ± s.e.m. Multiple comparisons, *p<0.05, **p<0.01, ***p<0.001, ****p<0.0001.

Enhancer RNAs are necessary for basal and stimulation-induced neuronal activity patterns

Enhancers have been demonstrated to be fundamental regulators of activity- and experience-dependent gene expression in the context of neuronal plasticity and memory formation (Joo et al., 2016; Kim et al., 2010; Malik et al., 2014; Schaukowitch et al., 2014; Telese et al., 2015). This regulatory role is in line with our data indicating that eRNAs are crucial regulators of activity-dependent gene transcription in cortical neurons, and further demonstrates the unidirectional nature of this mechanism. However, if and how active enhancers or even a single eRNA affect electrophysiological properties of neurons remains an open question. To investigate the significance of individual eRNAs in complex neuronal functions, we utilized multielectrode arrays (MEAs) to record neuronal activity in response to decreased (ASOs) *Fos* eRNA-1 levels. Rat primary cortical cultures grown on MEAs were treated with sequence-specific eRNA-1 ASOs or a scrambled control ASO for 24 hrs. Notably, firing patterns did not differ between wells prior to ASO treatment (Data not shown). Electrophysiological recordings were carried out for 20 min to establish a stable baseline, followed by a 10-min recording during which gabazine (GBZ), a $GABA_A$ antagonist, was added to neuronal culture media (**Fig. 7A**). ASO-mediated knock down of *Fos* eRNA-1 resulted in a robust decrease in action potential frequency (**Fig. 7D, F**) and number of action potential bursts, at baseline as well as in response to GBZ treatment (**Fig. 7E, G**). Intriguingly, we observed that by decreasing eRNA-1, we were able to block gabazine-induced changes in firing rates completely (**Fig. 7D**). Overall, these findings demonstrate that altering the levels of a single eRNA is sufficient to modulate neuronal communication, highlighting the importance of eRNAs not only in gene expression but also in neuronal function.

DISCUSSION

Distal enhancer elements in DNA enable higher-order chromatin interactions that facilitate gene expression programs and thus contribute to cellular phenotype and function (Heinz et al., 2015; Li et al., 2016; Wang et al., 2011). In the developing brain, the majority of enhancer elements exhibit temporally specific emergence during precise developmental windows, with only ~15% of enhancers being utilized continually from late embryonic development into adulthood (Gray et al., 2015; Nord et al., 2013). These developmentally regulated enhancers contribute to cell- and tissue-specific gene expression patterns that establish communication within and between brain structures (Frank et al., 2015; Nord et al., 2013; Pattabiraman et al., 2014). Not surprisingly, enhancers utilized in early embryonic brain development possess the highest degree of sequence conservation across species, suggesting that robust evolutionary pressures drive enhancer function (Nord et al., 2013). In the postnatal and mature brain, enhancers continue to play a widespread role in the activity-dependent transcriptional programs that regulate key aspects of neuronal plasticity and function (Gray et al., 2015; Hnisz et al., 2013; Joo et al., 2016; Kim et al., 2010; Malik et al., 2014; Telese et al., 2015; Vermunt et al., 2014). Repression or deletion of enhancer elements has profound effects on the genes that they control, including complete inactivation (Joo et al., 2016; Kearns et al., 2015; Malik et al., 2014; Telese et al., 2015). Likewise, targeted enhancer activation induces robust upregulation of linked genes, suggesting that enhancers serve as bidirectional regulators of gene activity (Frank et al., 2015; Hilton et al., 2015).

Although it is well accepted that genomic enhancers play critical roles in tuning the spatiotemporal nature of transcription from linked genes, techniques typically used to examine enhancer function (e.g., enhancer deletion (Leighton et al., 1995), Cas9-based mutation (Lopes et al., 2016; Sanjana et al., 2016), or activation/inactivation with dCas9 fusion proteins (Hilton et al., 2015; Joo et al., 2016; Liu et al., 2017; Liu et al., 2016)) interfere with both the genomic locus and eRNAs transcribed from that locus. Therefore, these approaches cannot dissociate the effects of enhancer function and eRNA function. To address this problem, we took two different approaches that directly target eRNAs in order to examine their function separately from enhancer function. First, we used a novel CRISPR-Display approach in neuronal cultures to target *Fos* eRNA to its own enhancer. These results demonstrate that *Fos* eRNA is sufficient to induce *Fos* mRNA. Secondly, we employed stable, cell-penetrating ASOs to target eRNA for degradation. These results suggest that eRNA is necessary for normal expression of *Fos* mRNA, both under basal conditions and after neuronal depolarization. Finally, our results show that altered levels of a single eRNA without any changes to the underlying enhancer sequence is sufficient to modulate neuronal firing patterns (**Fig. 7**). Together, these findings strongly support

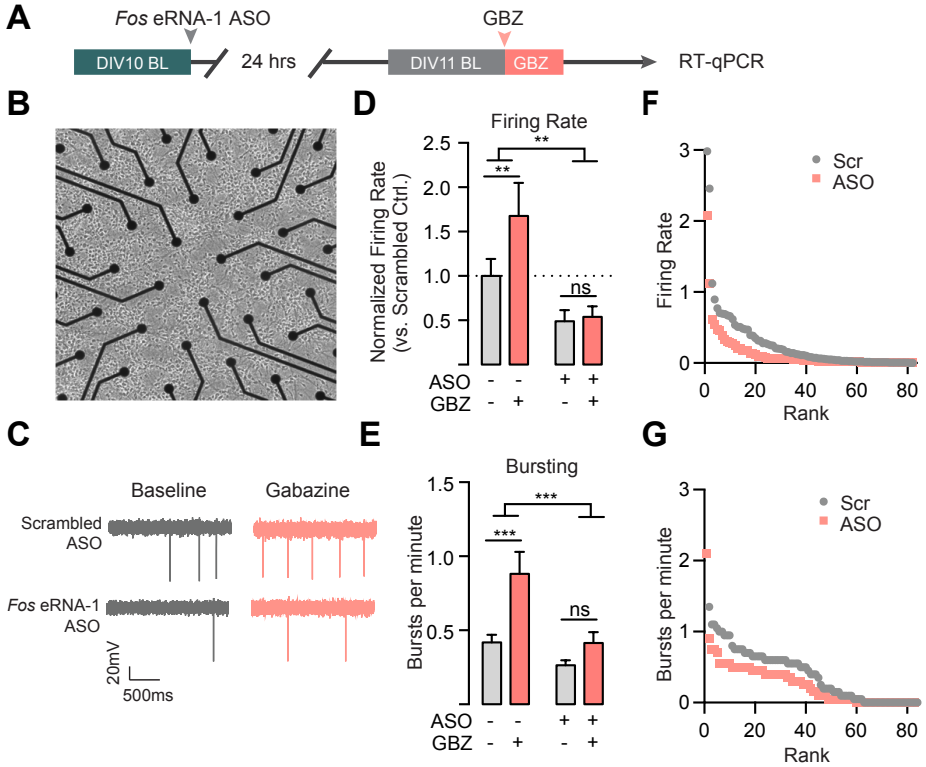

Figure 7. *Fos* eRNA-1 is necessary for normal neuronal activity at baseline and in response to activation. **A**, Timeline of recordings (boxes) and treatments (arrows). **B**, Primary neuronal cortex cultures grown on a multi electrode array (MEA) plate. **C**, Example traces of scrambled or eRNA-1 targeting ASO treated neurons at baseline and in response to treatment with 5 μM gabazine. **D-E**, ASO mediated decreases in *Fos* eRNA-1 levels result in lower firing rates at baseline, fewer bursts per minute, and prevent the response to gabazine treatment (two-way ANOVA, with main effect of ASO on firing rates $F(1,165)=8.345$, $p=0.0044$ and on bursting $F(1,332)=12.25$, $p=0.0005$, and with GBZ main effect on firing rates $F(1,165)=5.775$, $p=0.017$ and on bursting $F(1,332)=11.92$, $p=0.006$; Sidak's post hoc test for multiple comparison with Scrambled ASO n=85 and eRNA-1 ASO n=83). **F-G**, Ranked baseline firing rates and bursts per minute after scrambled ASO or eRNA-1 targeting ASO treatment indicate stronger ASO effects in highly active neurons. Data expressed as mean ± s.e.m. Multiple comparisons, *p<0.05, **p<0.01, ***p<0.001, ****p<0.0001.

a critical role for eRNAs in regulation of gene expression programs induced in response to neuronal activation.

Overall, these results are in agreement with a previous report demonstrating that eRNAs transcribed from activity-dependent enhancers are necessary for induction of mRNA from linked genes (Schaukowitch et al., 2014). This report utilized lentiviral shRNA knockdown approaches to directly target activity-induced eRNAs near *Arc* and *Gadd45b* genes, and followed this knockdown with KCl depolarization to induce mRNAs. Targeted shRNA knockdown of eRNA specifically blocked mRNA induction at these genes, but not other IEGs induced by neuronal activation (*Fos*, *Egr1*). Our results extend these important findings in two ways. First, given that the *Fos* gene exhibits multiple enhancers and activity-dependent eRNAs, we were able to address the functional relationship between eRNAs near the same gene. Our results suggest that while eRNAs do regulate mRNA induction at linked genes, eRNAs are functionally independent of each other. Thus, ASO-mediated knockdown of eRNAs transcribed from the most distal *Fos* enhancer did not downregulate eRNAs transcribed from other enhancers (**Fig. 6**). Secondly, in parallel experiments we were able to target *Fos* mRNA for knockdown using an identical approach. These results demonstrate that the relationship between eRNA and mRNA levels at the same gene is unidirectional – i.e., that mRNA knockdown does not also reduce eRNA levels. This is a critical control at IEGs like *Fos*, given that the protein product of this gene is a transcription factor that localizes to enhancers in an AP1 complex with Jun family members (Malik et al., 2014).

Biological roles of lncRNAs are generally linked to their ability to bind functionally active proteins to operate as molecular guides, decoy molecules, scaffolding, or even allosteric modulators (Quinn and Chang, 2016; Rinn and Chang, 2012). In agreement with this concept, a large number of chromatin associated proteins bind RNA in addition to DNA (Di Ruscio et al., 2013; Hendrickson et al., 2016; Savell et al., 2016), and several well-characterized transcriptional regulators have recently been shown to possess functional interactions with eRNAs (Bose et al., 2017; Hsieh et al., 2014; Lai et al., 2013; Li et al., 2013; Li et al., 2016; Schaukowitch et al., 2014; Sigova et al., 2015). For example, eRNAs interact with CREB binding protein (CBP) and stimulate its activity as a histone acetyltransferase at enhancer loci (Bose et al., 2017). Likewise, eRNAs have been shown to bind the ubiquitous transcription factor Yin-Yang 1 (YY1) to "trap" YY1 at the enhancer, thus facilitating its action at local YY1 motifs in DNA (Sigova et al., 2015). Finally, eRNAs can act as decoy molecules for negative elongation factor (NELF) complexes, which are important regulators of RNAP2 pausing and transcriptional bursting (Schaukowitch et al., 2014). While our results do not reveal how eRNA-protein interactions may direct enhancer functions in neurons, our results add to this existing evidence by showing that eRNAs transcribed from a single enhancer can exist at multiple locations in a nucleus and, when targeted to a specific enhancer using CRISPR-Display, are sufficient to regulate expression of linked genes. Future studies could explore which factors influence enhancer and eRNA function such as distance from their target gene, eRNA localization, eRNA length and sequence, and eRNA/protein interactions. This will help to determine whether common regulatory mechanisms dictate expression of eRNAs targeting the same gene. It will further help to investigate whether a group of eRNAs that regulate the same gene have distinct functional mechanisms. It will be crucial to understand the interplay of different enhancers and eRNAs and how they regulate gene expression and potentially fine-tune response to specific stimuli.

The vast majority of gene variants linked to human health and disease by genome-wide association studies are located in non-coding regions of the genome (Gordon and Lyonnet, 2014; Network and Pathway Analysis Subgroup of Psychiatric Genomics, 2015; Schizophrenia Working Group of the Psychiatric Genomics, 2014; Vermunt et al., 2014), with putative enhancers containing more disease-linked single-nucleotide polymorphisms than all other genetic loci combined (Corradin and Scacheri, 2014). Disease-linked genetic variants could affect enhancer activity either via direct modification of enhancer DNA sequence (e.g., disruption of a transcription factor motif), or by alterations

in long-range chromatin interactions between enhancers and gene promoters. Indeed, numerous diseases have already been linked to sequence variations in enhancer regions (Gordon and Lyonnet, 2014; Jeong et al., 2008; Spieler et al., 2014; Vermunt et al., 2014), including complex polygenic conditions such as depression (Davidson et al., 2011; Edwards et al., 2012), obesity (Davidson et al., 2011; Voisin et al., 2015), schizophrenia (Eckart et al., 2016; Roussos et al., 2014), bipolar disorder (Eckart et al., 2016), and autism spectrum disorders (Inoue and Inoue, 2016; Yao et al., 2015). This growing link between enhancer activity and brain function strongly highlights the need to better understand the mechanistic interactions that regulate enhancer function at the molecular level, and also suggests that enhancers could be attractive targets for a new generation of disease therapeutics.

METHODS

Genome-wide quantification and characterization of eRNA species. Identification and characterization of transcriptionally active enhancers was performed using previously published non-PolyA RNA-seq datasets (available under GEO accession number GSE64988) (Savell et al., 2016). This dataset was generated using rat DIV 11 cortical neuron cultures treated for 1 hr with vehicle, 25 mM KCl, or 1 μM TTX. Extracted RNA underwent two selection processes. First, polyadenylated (PolyA+) RNA was captured with the NEBNext Poly(A) mRNA Magnetic Isolation Module. Secondly, the remaining non-polyadenylated (non-PolyA) underwent ribosomal RNA depletion (NEBNext rRNA depletion kit) prior to directional, 50bp, paired-end sequencing on an Illumina HiSeq 2000 platform. Raw paired-end sequenced reads were quality controlled, filtered for read quality (FASTX toolkit, Galaxy) and aligned to the rat Rn5 genome sequence in Galaxy using Tophat v1.4.0. General analyses were performed in Seqmonk v1.38.2 (Babraham Institute), using a merged dataset of ~118 million mapped non-PolyA reads from six independent biological replicates (two per treatment group).

For genome-wide characterization of transcriptionally active enhancer elements and enhancer identification, we used an RNA-driven pipeline. Genome-aligned BAM files were probed for contiguously transcribed elements (>100bp, merging elements closer than 1kb) using reads on both strands. Using a 12x read depth cutoff, we identified 31,346 regions of contiguous transcription, of which 18,422 fell within 1kb or overlapped annotated genes. Due to the difficulty in separating intronic enhancers from potential promoters or other elements, these were removed from consideration. The 12,924 regions remaining were designated as transcribed intergenic regions (TIRs). Next, to capture TIRs that corresponded to enhancers, we filtered this list against overlapping histone modification peaks from adult mouse cortex (ENCODE project datasets obtained from the UCSC Table Browser and transformed from mm9 to Rn5 genome coordinates using Liftover). Of 12,924 TIRs, 22.5% overlapped H3K4me1 peaks, a mark commonly used to denote active enhancers. Likewise, an additional 5.2% of TIRs overlapped adult cortex H3K4me3 and H3K27ac, which are commonly used to mark poised enhancers. Together, this combination of 3,107 transcriptionally active enhancers (TAEs) was characterized for other key elements, including RNAP2 and CTCF binding (ENCODE project datasets obtained from the UCSC Table Browser and transformed from mm9 to Rn5 genome coordinates using Liftover), and sequence conservation (PhastCons13way species conserved element BED file) or CpG islands (both obtained from UCSC Table Browser using Rn5 genome coordinates).

For differential comparison of eRNA elements that are altered by neuronal depolarization (termed activity-responsive TAEs, or arTAEs), we quantified and compared read counts in Vehicle and KCl non-PolyA RNA-seq libraries at all 3,107 transcriptionally active enhancers using DESeq2 (Seqmonk wrapper for R; corrected for multiple comparisons, FDR = 0.05). Of 3,107 enhancer elements, 89 exhibited significant differential regulation by KCl depolarization. For quantification of mRNA transcripts at nearby genes, PolyA+ datasets from the same experiments were used to compute log2(fold change) for differentially expressed genes (230 differentially expressed genes identified using DESeq2, corrected for multiple comparisons, FDR = 0.05).

Gene ontology analysis of gene clusters identified in using this approach was performed using the ClueGO plugin in Cytoscape. Enrichment analysis was conducted using a reference set of all rat protein coding genes. Significantly enriched biological process terms (hierarchy level 8-15) containing at least 10% of genes in each category were identified using a Benjamini–Hochberg false-discovery rate and $\alpha = 0.05$.

Cultured neuron experiments. Primary rat cortical neuronal cultures were generated from embryonic day 18 rat cortical tissue as described previously (Day et al., 2013; Savell et al., 2016). Briefly, cell culture wells and MEAs were coated overnight at 37° C with poly-L-lysine (0.05 mg/ml for culture wells; 0.1 mg/ml supplemented with 0.01 mg/ml Laminin for MEAs) and rinsed with diH_2O. Dissected cortices were incubated with papain for 25 min at 37°C. After rinsing in Hank's Balanced Salt Solution (HBSS), a single cell suspension of the tissue was re-suspended in Neurobasal media (Invitrogen) by trituration through a series of large to small fire-polished Pasteur pipets. Primary neuronal cells passed through a 100 μM cell strainer, spun and re-suspended in fresh media. Cells were then counted and plated to a density of 100,000 cells per well on 6-well MEA plates, 125,000 cells per well on 24-well culture plate and 250,000 cells per well on 12-well culture plate with or without glass coverslips (60,000 cells/cm). Cells were grown in Neurobasal media plus B-27 and L-glutamine supplement (complete Neurobasal media) for 11 days in vitro in a humidified CO_2 (5%) incubator at 37° C. MEAs were switched to BrainPhys media (Stemcell Technologies Inc.) plus SM1 and L-glutamine supplement on DIV5.

At 4-11 days in vitro, neuronal cultures were treated as described. For KCl stimulation experiments, KCl (Sigma) was added to complete Neurobasal media (2X specified concentration), and half of the cell culture media (500 μl) was replaced with KCl solution or vehicle (complete Neurobasal media alone).

Cells were incubated with KCl for described time points prior to RNA extraction. For TTX inactivation experiments, cells were treated with 1 μM TTX (Tocris Bioscience) in Neurobasal media for the described time points prior to RNA extraction. S-AMPA, NMDA, and Forskolin (Sigma) were diluted in sterile water and added to cultures for 1 hr at a volume of 10 μl (final concentrations of 1 μM, 10 μM, or 100 μM). 10 μl sterile water was added as a vehicle control. For experiments involving RNAP inhibitors, cultures were treated for 4 hrs or 4 hrs followed

by a 1 hr, 25 mM KCl stimulation. The RNAP2-dependent transcriptional inhibitor DRB (Sigma) was dissolved to a 20 mM stock solution in 100% cell culture grade DMSO (Sigma) and diluted in Neurobasal media to described experimental concentrations. Vehicle treated cells received equal concentrations of DMSO in Neurobasal media. At a minimum, all cell culture experiments were performed in triplicate.

For viral transduction, cells were transduced with 5 µl virus on DIV 4 or 5 (minimum 3.97×10^8 IU/ml for a final MOI of 7.94). After an 8-12 hr incubation period, virus containing media was replaced with conditioned media to minimize toxicity. A regular half media change followed on DIV 8. On DIV 11 transduced cells were imaged and virus expression was verified prior to KCl-treatment and/or RNA extraction. IHC for GFP or FLAG was performed as described previously (Savell et al., 2016), with monoclonal anti-GFP (MAB3580, Millipore, RRID:AB_94936) or anti-FLAG (MA1-91878, Thermo Fisher Scientific, RRID: AB_1957945) antibodies.

RNA extraction and RT-qPCR. Total RNA was extracted (RNAeasy kit, Qiagen) with DNase treatment (RNase free DNAse, Qiagen), and reverse-transcribed (iScript cDNA Synthesis Kit, Bio- Rad). cDNA was subject to RT-PCR for genes of interest, as described previously (Savell et al., 2016). A list of PCR primer sequences is provided in **Supplementary Data Table 3**.

Chromatin immunoprecipitation (ChIP). Following KCl stimulation, neuronal cultures (~3,000,000 million cortical neurons per treatment group) were fixed with 1% paraformaldehyde in 1x PBS plus Halt Inhibitor Cocktail (ThermoFisher) and washed with 1x PBS. Cells were then extracted and lysed in Lysis Buffer (50 mM HEPES, 10 mM NaCl, 1 mM EDTA, 0.5% NP-40, Halt Cocktail), spun down, and resuspended in 100 µl of RIPA Buffer (1% NP-40, 1% SDS, HALT Cocktail in 1x PBS). Following resuspension, each sample was sheared via sonication (BioRuptor Pico) and spun down once again to remove debris. The resulting supernatant was diluted to 1 ml using RIPA buffer and aliquoted into input and IP samples. Immunoprecipitation was performed with a RNAP2 antibody (Active Motif, 39097). Antibody-protein complexes were isolated with magnetic beads (Dynabeads protein A, Invitrogen). Each sample was incubated overnight at 4°C. Following incubation, all samples were washed sequentially with Low-salt immune complex buffer (Millipore), High-salt immune complex buffer (Millipore), LiCl immune complex buffer (Millipore), and Tris-EDTA (TE) buffer (Fisher Scientific). To revert protein-DNA crosslinks, samples were resuspended in TE buffer plus 1% SDS, RNase, and Proteinase K and incubated for 2 hrs at 65°C. The resultant DNA was then purified using a PCR cleanup kit (Qiagen), and levels of protein-DNA interactions were measured using qPCR.

CRISPR-dCas9 construct design. To achieve transcriptional activation, lentivirus-compatible plasmids were engineered to express dCas9 fused to VP64, VPR, or p300 constructs. dCAS9-VP64_GFP was a gift from Feng Zhang (Addgene plasmid # 61422 (Konermann et al., 2015)). SP-dCas9-VPR was a gift from George Church (Addgene plasmid # 63798 (Chavez et al., 2015)), which was edited by insertion of the dCas9-VPR cassette into a lentivirus-compatible backbone and insertion of an hSyn promoter for robust neuronal expression. The pcDNA-dCas9-p300 Core construct was a gift from Charles Gersbach (Addgene plasmid # 61357 (Hilton et al., 2015)). VP64 and VPR expressing constructs were co-transduced with gRNA containing constructs. Gene-specific gRNAs were designed using an online gRNA tool, provided by the Zhang Lab at MIT (crispr.mit.edu). To ensure specificity all CRISPR crRNA sequences were analyzed with BLAST. gRNAs were designed to target *Fos*, *Fosb*, and *Nr4a1* enhancers respectively, as well as the promoter regions (a list of the target sequences is provided in **Supplementary Data Table 3**). crRNA sequences were annealed and ligated into the gRNA scaffold using the BsmBI cut site. Plasmids were sequence-verified with Sanger sequencing. For CRISPR-Display, lentiCRISPR v2 from Feng Zhang (Addgene plasmid # 52961 (Sanjana et al., 2014)) was modified, and engineered to express dCas9 (instead of Cas9), gRNA, an 100bp sequence of eRNA-1 and GFP via restriction enzyme cloning using gBlocks for eRNA-1 (cut with SwaI and EcoRI) and GFP (cut with MluI and BamHI) respectively. As a control, a plasmid lacking the eRNA sequence was targeted to the same genomic sites.

C6 Cell Culturing and Nucleofection. C6 cells were obtained from American Type Culture Collection (CCL-107, ATCC, RRID:CVCL_0194) and cultured in F-12k based medium (2.5% bovine serum, 12% horse serum). At each passage, cells were trypsinized for 1-3 min (0.25% trypsin and 1 mM EDTA in PBS pH 7.4) at room temperature. After each passage remaining cells were processed for nucleofection (2×10^6/group). Cell pellets were resuspended in nucleofection buffer (5 mM KCl, 15 mM MgCl, 15 mM HEPES, 125 mM Na_2HPO_4/NaH_2PO_4, 25 mM Mannitol) and electroporated with 3.4µg plasmid DNA per group. Nucleofector™2b device (Lonza) was used according to the manufacturer's instruction (C6, high efficiency protocol). Nucleofection groups were diluted with 500 µl media respectively and plated in triplicates in 24-well plates (~ 666,667 cells/well). Plates underwent a full media change 4-6 hrs after nucleofection, and were imaged and frozen for downstream processing after 16 hrs.

Lentivirus production. Viruses were produced in a sterile environment subject to BSL-2 safety by transfecting HEK-293T cells with specified CRISPR-dCas9 plasmids, the psPAX2 packaging plasmid, and the pCMV-VSV-G envelope plasmid (Addgene 12260 & 8454) with FuGene HD (Promega) for 40 hrs. Viruses were purified using filter (0.45 mm) and ultracentrifugation (25,000 rpm, 1 hr 45 min) steps. Viral titer was determined using a qPCR Lentivirus Titration Kit (Applied Biological Materials). Viruses were stored in sterile PBS at -80°C.

Antisense oligonucleotide (ASO) design and treatment. To manipulate *Fos* mRNA or eRNA levels, we designed 20 bp ASOs that targeted distinct transcripts from the Fos gene locus (see **Supplementary Data Table 3** for target sequences). ASOs targeting exon 3 of *Fos* mRNA or *Fos* eRNA-1 were synthesized with two chemical modifications: an all phosphorothioate backbone and five 2' O-methyl RNA bases on each end of the oligonucleotide (Integrated DNA Technologies). Primary neuronal cultures were treated with scrambled or *Fos* targeted ASOs (15 µM in buffer EB, for a final concentration of 1.5 µM) and incubated for 24 hrs (basal experiments) or 1 hr neuronal depolarization with 25 mM KCl (or vehicle control). Following ASO treatment,

RNA was extracted (Qiagen RNeasy kit) and *Fos* mRNA and eRNA levels were determined using RT-qPCR with custom primers.

Single Molecule RNA FISH.

smFISH Probe Design. We designed and ordered Stellaris® FISH probe sets for *Gapdh* mRNA, *Fos* eRNA-1, *Fos* eRNA-3 and *Fos* mRNA carrying a fluorophore (Quasar® 570 for eRNA-1 and *Gapdh* mRNA probes, Quasar® 670 for eRNA-3 and both *Fos* and *Gapdh* mRNA probes). We preferred probes of 20-mer oligonucleotides. Multiple probes per set targeting the same RNA molecule were designed for an adequate signal to background ratio and to optimize signal strength. Target sequences of each probe set are provided in **Supplementary Data Table 3**).

Sample Preparation and Hybridization. Day 1: Primary neuronal cultures (~250,000 neurons per coverslip/well) were KCl or Vehicle treated for 1 hr on DIV 11. After treatment cells were cross-linked with 3.7% formaldehyde (paraformaldehyde in 1X PBS) for 10 min at room temperature (21°C) on a rocking platform. Wells were washed twice with PBS and permeabilized in 70% ethanol for at least 3 hrs at 4°C. Wells were washed in Stellaris® Wash Buffer A with for 5 min at room temperature. Coverslips were transferred to a humidifying chamber and incubated with hybridization buffer (0.5 nM mRNA probe, 0.5 nM eRNA probe) for 14 hrs at 37°C. Day 2: Coverslips were washed three times in Stellaris® Wash Buffer A for 30 min at 37°C. After a 5 min wash in Stellaris® Wash Buffer B at room temperature, coverslips were mounted using ProLong™ antifade with DAPI for imaging.

Quantification of Expression. A number of freely available programs have been developed to quantify smRNA FISH results. We used StarSearch (http://rajlab.seas.upenn.edu/StarSearch/launch.html), which was developed by Marshall J. Levesque and Arjun Raj at the University of Pennsylvania to automatically count individual RNAs. mRNA and eRNA detection involved two major steps. First, images for each probe set as well as a DAPI image are merged and cells were outlined. Punctae detection was carried out and additional adjustment of thresholds was performed. The same threshold range was used for all images, and this analysis was performed blind to treatment group. As a negative control, we quantified processed samples without FISH probes to determine non-specific background signals. Background signal for the Quasar® 570 channel (which was used to image *Fos* eRNA-1 and *Gapdh* mRNA) was close to zero (0.3761 ± 0.07906 spots/cell). We did not detect any background spots in the Quasar® 670 channel, which was used to image *Fos* mRNA, eRNA-3, and *Gapdh* mRNA.

Multi Electrode Array Recordings.

Electrophysiological activity of single neurons was recorded using a MEA2100 Lite recording system (Multi Channel Systems). E18 rat primary cortical neurons were plated in 6-well multielectrode arrays, as described above. Each MEA well contained 9 extracellular recording electrodes and a dedicated ground electrode. During recording sessions, MEAs were connected to a temperature-controlled headstage (monitored at 37°C) containing a 60-bit amplifier. Electrical activity was sampled by an interface board at 30 kHz, digitized, and transmitted to an external PC for data acquisition and analysis in MC Rack software (Multi Channel Systems). All data were filtered using dual 10Hz (high pass) and 10,000Hz (low-pass) Butterworth filters. Action potential thresholds were set manually for each electrode (typically > 4 standard deviations from the mean signal). Neuronal waveforms collected in MC Rack were then exported to Offline Sorter (Plexon) for further waveform analysis, separation of distinct waveforms corresponding to multiple units on one electrode channel, and confirmation of waveform isolation using principal component analysis, inter-spike intervals, and auto- or cross-correlograms. Further analysis of burst activity and firing rate was performed in NeuroExplorer. Recording sessions consisted of a 30-minute recording window on DIV11. Neuronal activity was sampled for 20 min on at baseline, followed by a 10-min recording with 5 μM Gabazine treatment. For comparison, spontaneous activity was also recorded prior to eRNA-1 targeting ASO or scrambled ASO treatment on DIV10.

Statistical Analysis. Transcriptional differences from PCR experiments were compared with one-way ANOVA with Dunnett's post-hoc tests, or Mann-Whitney test where appropriate. Significance of smFISH data was assessed with Mann-Whitney test or Pearson correlation test. Statistical significance was designated at $\alpha = 0.05$ for all analyses. Statistical and graphical analyses were performed with Graphpad software (Prism). Statistical assumptions (e.g., normality and homogeneity for parametric tests) were formally tested and boxplots were examined.

AUTHOR CONTRIBUTIONS

N.V.N.C, R.C.S, and J.J.D conceived of these experiments, performed experiments, and wrote the manuscript. J.S.R., K.D.B., A.S., K.E.S., and F.A.S assisted in experiments. N.V.N.C, R.C.S, and J.J.D performed bioinformatics analysis. J.J.D. supervised all work.

ACKNOWLEDGEMENTS

We acknowledge the Civitan International Research Center Cellular Imaging Facility. This work was supported by NIH grants DA039650, DA034681, and MH114990 and the UAB Pittman Scholar Program (JJD), DA042514 (K.E.S.), DA041778 (F.A.S.), and the CIRC Emerging Scholar Award (NVNC).

REFERENCES

Arner, E., Daub, C.O., Vitting-Seerup, K., Andersson, R., Lilje, B., Drablos, F., Lennartsson, A., Ronnerblad, M., Hrydziuszko, O., Vitezic, M., et al. (2015). Transcribed enhancers lead waves of coordinated transcription in transitioning mammalian cells. Science 347, 1010-1014.

Bose, D.A., Donahue, G., Reinberg, D., Shiekhattar, R., Bonasio, R., and Berger, S.L. (2017). RNA Binding to CBP Stimulates Histone Acetylation and Transcription. Cell 168, 135-149 e122.

Chavez, A., Scheiman, J., Vora, S., Pruitt, B.W., Tuttle, M., E, P.R.I., Lin, S., Kiani, S., Guzman, C.D., Wiegand, D.J., et al. (2015). Highly efficient Cas9-mediated transcriptional programming. Nat Methods 12, 326-328.

Corradin, O., and Scacheri, P.C. (2014). Enhancer variants: evaluating functions in common disease. Genome Med 6, 85.

Davidson, S., Lear, M., Shanley, L., Hing, B., Baizan-Edge, A., Herwig, A., Quinn, J.P., Breen, G., McGuffin, P., Starkey, A., et al. (2011). Differential activity by polymorphic variants of a remote enhancer that supports galanin expression in the hypothalamus and amygdala: implications for obesity,

depression and alcoholism. Neuropsychopharmacology 36, 2211-2221.

Day, J.J., Childs, D., Guzman-Karlsson, M.C., Kibe, M., Moulden, J., Song, E., Tahir, A., and Sweatt, J.D. (2013). DNA methylation regulates associative reward learning. Nat Neurosci 16, 1445-1452.

Di Ruscio, A., Ebralidze, A.K., Benoukraf, T., Amabile, G., Goff, L.A., Terragni, J., Figueroa, M.E., De Figueiredo Pontes, L.L., Alberich-Jorda, M., Zhang, P., et al. (2013). DNMT1-interacting RNAs block gene-specific DNA methylation. Nature 503, 371-376.

Djebali, S., Davis, C.A., Merkel, A., Dobin, A., Lassmann, T., Mortazavi, A., Tanzer, A., Lagarde, J., Lin, W., Schlesinger, F., et al. (2012). Landscape of transcription in human cells. Nature 489, 101-108.

Eckart, N., Song, Q., Yang, R., Wang, R., Zhu, H., McCallion, A.S., and Avramopoulos, D. (2016). Functional Characterization of Schizophrenia-Associated Variation in CACNA1C. PLoS One 11, e0157086.

Edwards, A.C., Aliev, F., Bierut, L.J., Bucholz, K.K., Edenberg, H., Hesselbrock, V., Kramer, J., Kuperman, S., Nurnberger, J.I., Jr., Schuckit, M.A., et al. (2012). Genome-wide association study of comorbid depressive syndrome and alcohol dependence. Psychiatr Genet 22, 31-41.

Fleischmann, A., Hvalby, O., Jensen, V., Strekalova, T., Zacher, C., Layer, L.E., Kvello, A., Reschke, M., Spanagel, R., Sprengel, R., et al. (2003). Impaired long-term memory and NR2A-type NMDA receptor-dependent synaptic plasticity in mice lacking c-Fos in the CNS. J Neurosci 23, 9116-9122.

Frank, C.L., Liu, F., Wijayatunge, R., Song, L., Biegler, M.T., Yang, M.G., Vockley, C.M., Safi, A., Gersbach, C.A., Crawford, G.E., et al. (2015). Regulation of chromatin accessibility and Zic binding at enhancers in the developing cerebellum. Nat Neurosci 18, 647-656.

Gordon, C.T., and Lyonnet, S. (2014). Enhancer mutations and phenotype modularity. Nat Genet 46, 3-4.

Gray, J.M., Kim, T.K., West, A.E., Nord, A.S., Markenscoff-Papadimitriou, E., and Lomvardas, S. (2015). Genomic Views of Transcriptional Enhancers: Essential Determinants of Cellular Identity and Activity-Dependent Responses in the CNS. J Neurosci 35, 13819-13826.

Hangauer, M.J., Vaughn, I.W., and McManus, M.T. (2013). Pervasive transcription of the human genome produces thousands of previously unidentified long intergenic noncoding RNAs. PLoS Genet 9, e1003569.

Heinz, S., Romanoski, C.E., Benner, C., and Glass, C.K. (2015). The selection and function of cell type-specific enhancers. Nat Rev Mol Cell Biol 16, 144-154.

Hendrickson, D., Kelley, D.R., Tenen, D., Bernstein, B., and Rinn, J.L. (2016). Widespread RNA binding by chromatin-associated proteins. Genome Biol 17, 28.

Hilton, I.B., D'Ippolito, A.M., Vockley, C.M., Thakore, P.I., Crawford, G.E., Reddy, T.E., and Gersbach, C.A. (2015). Epigenome editing by a CRISPR-Cas9-based acetyltransferase activates genes from promoters and enhancers. Nat Biotechnol 33, 510-517.

Hnisz, D., Abraham, B.J., Lee, T.I., Lau, A., Saint-Andre, V., Sigova, A.A., Hoke, H.A., and Young, R.A. (2013). Super-enhancers in the control of cell identity and disease. Cell 155, 934-947.

Hsieh, C.L., Fei, T., Chen, Y., Li, T., Gao, Y., Wang, X., Sun, T., Sweeney, C.J., Lee, G.S., Chen, S., et al. (2014). Enhancer RNAs participate in androgen receptor-driven looping that selectively enhances gene activation. Proc Natl Acad Sci U S A 111, 7319-7324.

Inoue, Y.U., and Inoue, T. (2016). Brain enhancer activities at the gene-poor 5p14.1 autism-associated locus. Sci Rep 6, 31227.

Jeong, Y., Leskow, F.C., El-Jaick, K., Roessler, E., Muenke, M., Yocum, A., Dubourg, C., Li, X., Geng, X., Oliver, G., et al. (2008). Regulation of a remote Shh forebrain enhancer by the Six3 homeoprotein. Nat Genet 40, 1348-1353.

Joo, J.Y., Schaukowitch, K., Farbiak, L., Kilaru, G., and Kim, T.K. (2016). Stimulus-specific combinatorial functionality of neuronal c-fos enhancers. Nat Neurosci 19, 75-83.

Kaikkonen, M.U., Spann, N.J., Heinz, S., Romanoski, C.E., Allison, K.A., Stender, J.D., Chun, H.B., Tough, D.F., Prinjha, R.K., Benner, C., et al. (2013). Remodeling of the enhancer landscape during macrophage activation is coupled to enhancer transcription. Mol Cell 51, 310-325.

Kearns, N.A., Pham, H., Tabak, B., Genga, R.M., Silverstein, N.J., Garber, M., and Maehr, R. (2015). Functional annotation of native enhancers with a Cas9-histone demethylase fusion. Nat Methods 12, 401-403.

Kim, T.K., Hemberg, M., and Gray, J.M. (2015). Enhancer RNAs: a class of long noncoding RNAs synthesized at enhancers. Cold Spring Harb Perspect Biol 7, a018622.

Kim, T.K., Hemberg, M., Gray, J.M., Costa, A.M., Bear, D.M., Wu, J., Harmin, D.A., Laptewicz, M., Barbara-Haley, K., Kuersten, S., et al. (2010). Widespread transcription at neuronal activity-regulated enhancers. Nature 465, 182-187.

Kim, T.K., and Shiekhattar, R. (2015). Architectural and Functional Commonalities between Enhancers and Promoters. Cell 162, 948-959.

Konermann, S., Brigham, M.D., Trevino, A.E., Joung, J., Abudayyeh, O.O., Barcena, C., Hsu, P.D., Habib, N., Gootenberg, J.S., Nishimasu, H., et al. (2015). Genome-scale transcriptional activation by an engineered CRISPR-Cas9 complex. Nature 517, 583-588.

Lai, F., Orom, U.A., Cesaroni, M., Beringer, M., Taatjes, D.J., Blobel, G.A., and Shiekhattar, R. (2013). Activating RNAs associate with Mediator to enhance chromatin architecture and transcription. Nature 494, 497-501.

Leighton, P.A., Saam, J.R., Ingram, R.S., Stewart, C.L., and Tilghman, S.M. (1995). An enhancer deletion affects both H19 and Igf2 expression. Genes & development 9, 2079-2089.

Li, W., Notani, D., Ma, Q., Tanasa, B., Nunez, E., Chen, A.Y., Merkurjev, D., Zhang, J., Ohgi, K., Song, X., et al. (2013). Functional roles of enhancer RNAs for oestrogen-dependent transcriptional activation. Nature 498, 516-520.

Li, W., Notani, D., and Rosenfeld, M.G. (2016). Enhancers as non-coding RNA transcription units: recent insights and future perspectives. Nat Rev Genet 17, 207-223.

Liu, S.J., Horlbeck, M.A., Cho, S.W., Birk, H.S., Malatesta,

M., He, D., Attenello, F.J., Villalta, J.E., Cho, M.Y., Chen, Y., et al. (2017). CRISPRi-based genome-scale identification of functional long noncoding RNA loci in human cells. Science 355.

Liu, S.J., Nowakowski, T.J., Pollen, A.A., Lui, J.H., Horlbeck, M.A., Attenello, F.J., He, D., Weissman, J.S., Kriegstein, A.R., Diaz, A.A., et al. (2016). Single-cell analysis of long non-coding RNAs in the developing human neocortex. Genome Biol 17, 67.

Lopes, R., Korkmaz, G., and Agami, R. (2016). Applying CRISPR-Cas9 tools to identify and characterize transcriptional enhancers. Nat Rev Mol Cell Biol 17, 597-604.

Malik, A.N., Vierbuchen, T., Hemberg, M., Rubin, A.A., Ling, E., Couch, C.H., Stroud, H., Spiegel, I., Farh, K.K., Harmin, D.A., et al. (2014). Genome-wide identification and characterization of functional neuronal activity-dependent enhancers. Nat Neurosci 17, 1330-1339.

Network, and Pathway Analysis Subgroup of Psychiatric Genomics, C. (2015). Psychiatric genome-wide association study analyses implicate neuronal, immune and histone pathways. Nat Neurosci 18, 199-209.

Nord, A.S., Blow, M.J., Attanasio, C., Akiyama, J.A., Holt, A., Hosseini, R., Phouanenavong, S., Plajzer-Frick, I., Shoukry, M., Afzal, V., et al. (2013). Rapid and pervasive changes in genome-wide enhancer usage during mammalian development. Cell 155, 1521-1531.

Pattabiraman, K., Golonzhka, O., Lindtner, S., Nord, A.S., Taher, L., Hoch, R., Silberberg, S.N., Zhang, D., Chen, B., Zeng, H., et al. (2014). Transcriptional regulation of enhancers active in protodomains of the developing cerebral cortex. Neuron 82, 989-1003.

Quinn, J.J., and Chang, H.Y. (2016). Unique features of long non-coding RNA biogenesis and function. Nat Rev Genet 17, 47-62.

Rinn, J.L., and Chang, H.Y. (2012). Genome regulation by long noncoding RNAs. Annu Rev Biochem 81, 145-166.

Roussos, P., Mitchell, A.C., Voloudakis, G., Fullard, J.F., Pothula, V.M., Tsang, J., Stahl, E.A., Georgakopoulos, A., Ruderfer, D.M., Charney, A., et al. (2014). A role for noncoding variation in schizophrenia. Cell Rep 9, 1417-1429.

Sanjana, N.E., Shalem, O., and Zhang, F. (2014). Improved vectors and genome-wide libraries for CRISPR screening. Nat Methods 11, 783-784.

Sanjana, N.E., Wright, J., Zheng, K., Shalem, O., Fontanillas, P., Joung, J., Cheng, C., Regev, A., and Zhang, F. (2016). High-resolution interrogation of functional elements in the noncoding genome. Science 353, 1545-1549.

Sanyal, A., Lajoie, B.R., Jain, G., and Dekker, J. (2012). The long-range interaction landscape of gene promoters. Nature 489, 109-113.

Savell, K.E., Gallus, N.V., Simon, R.C., Brown, J.A., Revanna, J.S., Osborn, M.K., Song, E.Y., O'Malley, J.J., Stackhouse, C.T., Norvil, A., et al. (2016). Extra-coding RNAs regulate neuronal DNA methylation dynamics. Nat Commun 7, 12091.

Schaukowitch, K., Joo, J.Y., Liu, X., Watts, J.K., Martinez, C., and Kim, T.K. (2014). Enhancer RNA facilitates NELF release from immediate early genes. Mol Cell 56, 29-42.

Schizophrenia Working Group of the Psychiatric Genomics, C. (2014). Biological insights from 108 schizophrenia-associated genetic loci. Nature 511, 421-427.

Shechner, D.M., Hacisuleyman, E., Younger, S.T., and Rinn, J.L. (2015). Multiplexable, locus-specific targeting of long RNAs with CRISPR-Display. Nat Methods 12, 664-670.

Sigova, A.A., Abraham, B.J., Ji, X., Molinie, B., Hannett, N.M., Guo, Y.E., Jangi, M., Giallourakis, C.C., Sharp, P.A., and Young, R.A. (2015). Transcription factor trapping by RNA in gene regulatory elements. Science 350, 978-981.

Spieler, D., Kaffe, M., Knauf, F., Bessa, J., Tena, J.J., Giesert, F., Schormair, B., Tilch, E., Lee, H., Horsch, M., et al. (2014). Restless legs syndrome-associated intronic common variant in Meis1 alters enhancer function in the developing telencephalon. Genome research 24, 592-603.

Telese, F., Ma, Q., Perez, P.M., Notani, D., Oh, S., Li, W., Comoletti, D., Ohgi, K.A., Taylor, H., and Rosenfeld, M.G. (2015). LRP8-Reelin-Regulated Neuronal Enhancer Signature Underlying Learning and Memory Formation. Neuron 86, 696-710.

Vermunt, M.W., Reinink, P., Korving, J., de Bruijn, E., Creyghton, P.M., Basak, O., Geeven, G., Toonen, P.W., Lansu, N., Meunier, C., et al. (2014). Large-scale identification of coregulated enhancer networks in the adult human brain. Cell Rep 9, 767-779.

Voisin, S., Almen, M.S., Zheleznyakova, G.Y., Lundberg, L., Zarei, S., Castillo, S., Eriksson, F.E., Nilsson, E.K., Bluher, M., Bottcher, Y., et al. (2015). Many obesity-associated SNPs strongly associate with DNA methylation changes at proximal promoters and enhancers. Genome Med 7, 103.

Wang, D., Garcia-Bassets, I., Benner, C., Li, W., Su, X., Zhou, Y., Qiu, J., Liu, W., Kaikkonen, M.U., Ohgi, K.A., et al. (2011). Reprogramming transcription by distinct classes of enhancers functionally defined by eRNA. Nature 474, 390-394.

Yao, P., Lin, P., Gokoolparsadh, A., Assareh, A., Thang, M.W., and Voineagu, I. (2015). Coexpression networks identify brain region-specific enhancer RNAs in the human brain. Nat Neurosci 18, 1168-1174.

Zovkic, I.B., Paulukaitis, B.S., Day, J.J., Etikala, D.M., and Sweatt, J.D. (2014). Histone H2A.Z subunit exchange controls consolidation of recent and remote memory. Nature 515, 582-586.

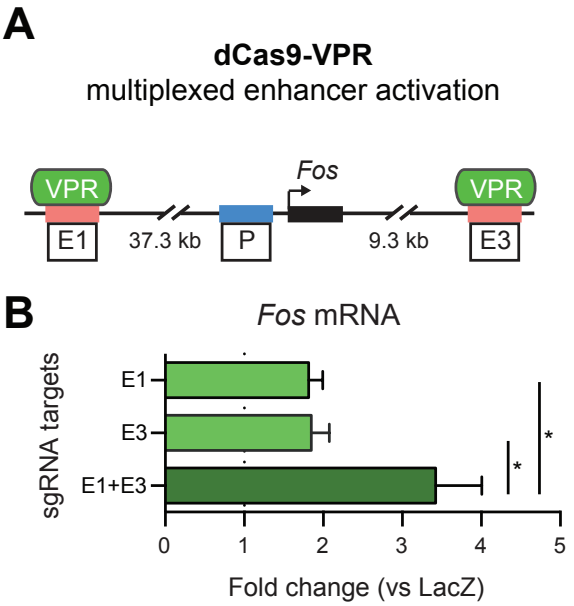

Supplementary Figure 1. Multiplexed enhancer activation. **A**, Illustration of CRISPRa targeting of transcriptional activator VPR to two *Fos* enhancer sites. **B**, RT-qPCR analysis of multiplexed activation of enhancer-1 and -3 reveals synergistic effects of dual enhancer activation and stronger *Fos* mRNA induction compared to individual enhancer activation (n=9 per group; one-way ANOVA for mRNA ($F(3,27)=9.527$, $p<0.01$; Kruskal-Wallis's multiple comparisons test),. Data expressed as mean ± s.e.m. Multiple comparisons, *$p<0.05$, **$p<0.01$, ***$p<0.001$, ****$p<0.0001$.

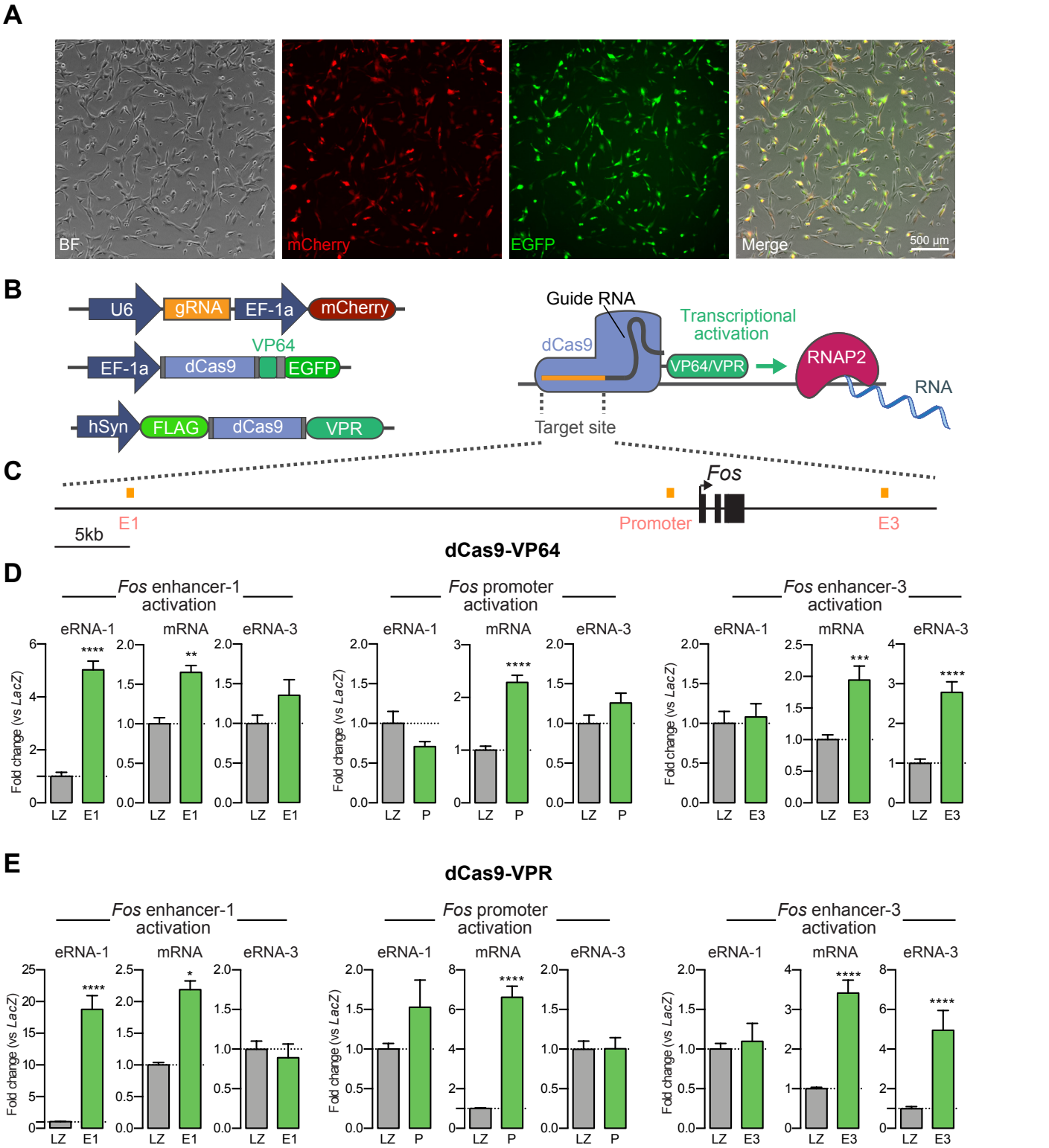

Supplementary Figure 2. Enhancer activation increases Fos eRNA and mRNA expression. **A**, C6 cells 16h post nucleofection with VP64 containing plasmids (dCas-VP64 expression marked by GFP reporter, gRNA expression marked by mCherry reporter). **B**, Illustration of CRISPR activation (CRISPRa) strategy for site-specific targeting of the transcriptional activator VP64. **C**, Target sites of gRNAs at 3 *Fos* enhancers, and one *Fos* promoter site. **D**, RT-qPCR analysis of VP64 mediated induction of *Fos* eRNAs and mRNA when targeted to individual sites surrounding the *Fos* gene, compared to the non-targeting *lacZ* control. CRISPRa resulted in site-specific upregulation of selected eRNAs and mRNA. Increasing *Fos* eRNA-1 and eRNA-3 levels resulted in increased *Fos* mRNA levels but not vice versa (n=9 per group; one-way ANOVA for eRNA-1 ($F(4,40)=66.22$, $p<0.0001$), eRNA-2 ($F(4,40)=22.85$, $p<0.0001$), eRNA-3 ($F(4,40)=10.55$, $p<0.0001$), and mRNA ($F(4,40)=14.66$, $p<0.0001$); Dunnett's multiple comparisons test). **E**, RT-qPCR analysis of VPR mediated induction of *Fos* eRNAs and mRNA when targeted to individual sites. CRISPRa resulted in site specific up-regulation of selected eRNAs and mRNA compared to non-targeting *lacZ* control (n=9 per group; one-way ANOVA for eRNA-1 ($F(4,40)=49.47$, $p<0.0001$), eRNA-2 ($F(4,40)=12.58$, $p<0.0001$),eRNA-3 ($F(4,40)=18.52$, $p<0.0001$), and mRNA ($F(4,40)=46.43$, $p<0.0001$); Dunnett's multiple comparisons test. Increasing *Fos* eRNA1 and eRNA-3 levels resulted in increased mRNA levels but not vice versa. Data expressed as mean ± s.e.m. Multiple comparisons, *$p<0.05$, **$p<0.01$, ***$p<0.001$, ****$p<0.0001$.

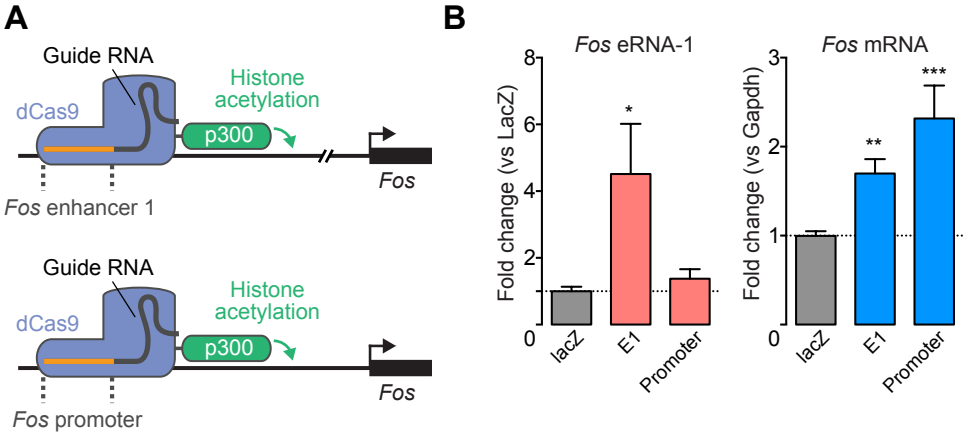

Supplementary Figure 3. Targeted histone acetlyation activates enhancer regions and yields increased eRNA and mRNA expression in C6 cells. **A**, Illustration of CRISPR-dCas9 strategy using a histone acetyl-transferase (p300) containing construct. **B**, RT-qPCR analysis of p300 mediated induction of *Fos* eRNA-1 and mRNA when targeted to individual sites (*lacZ*, *Fos* enhancer-1 or *Fos* promoter). CRISPRa resulted in site specific upregulation of selected eRNAs and mRNA (n=9 per group; Kruskal-Wallis for eRNA1 ($H(2)=15.00$, $p<0.05$), mRNA ($H(2)=7.825$ $p=0.001$). Targeting and increasing *Fos* eRNA-1 expression resulted in increased mRNA levels but not vice versa (Kruskal-Wallis for E1 ($H(2)=15.00$, $p<0.001$); Dunnett's multiple comparisons test. Data expressed as mean ± s.e.m. Multiple comparisons, *$p<0.05$, **$p<0.01$, ***$p<0.001$, ****$p<0.0001$.

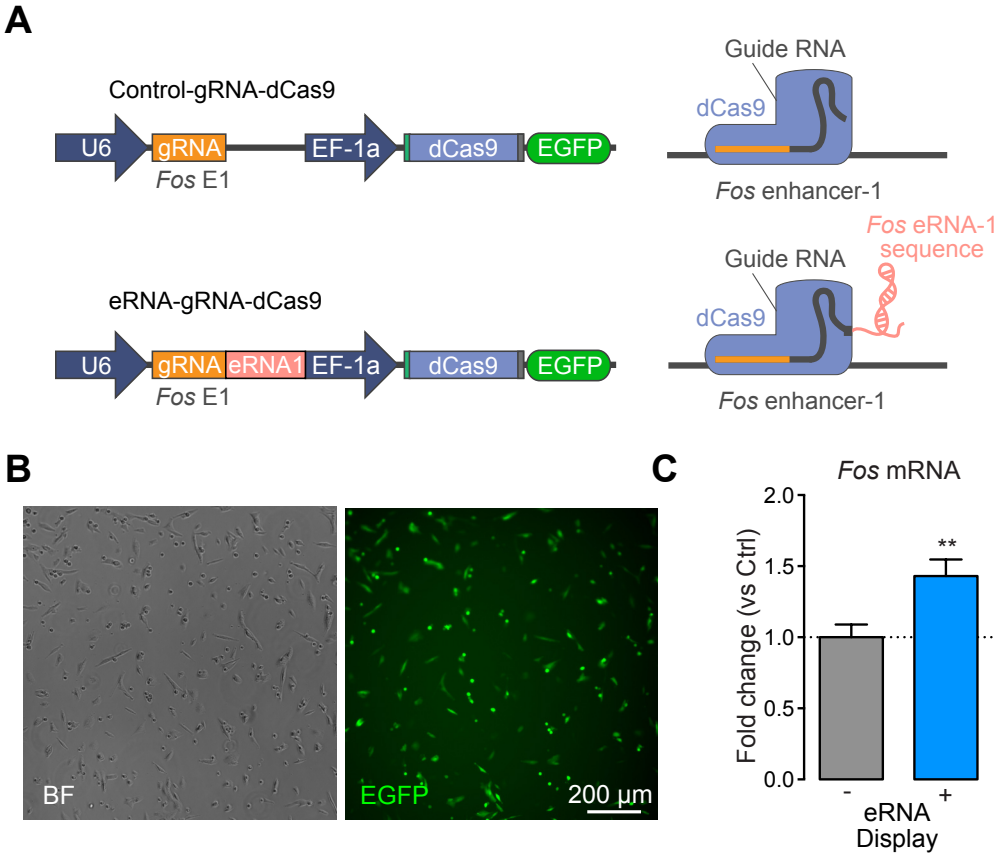

Supplementary Figure 4. eRNA-1 targeting to enhancer-1 is sufficient to induce *Fos* mRNA in C6 cells. **A**, Illustration of CRISPR-Display strategy for eRNA localization to enhancer-1. eRNA sequence is expressed with specific guide RNAs to target selected enhancers. **B**, C6 cells 16h post nucleofection with eRNA-1 CRISPR-Display construct. **C**, RT-qPCR analysis reveals that targeting eRNA-1 to enhancer-1 results in increased *Fos* mRNA expression (n=9 per group, unpaired Student's t-test t(16)=2.922, p=0.01. Data expressed as mean ± s.e.m. Multiple comparisons, *p<0.05, **p<0.01, ***p<0.001, ****p<0.0001.